Exploring the influence of precipitation extremes and human water use on total water storage (TWS) changes in the Ganges-Brahmaputra-Meghna River Basin

Water Resources Research, 2016

Exploring the influence of precipitation extremes and human water use on total water storage (TWS) changes in the Ganges-Brahmaputra-Meghna River Basin

Khandu,[1,2] Ehsan Forootan,[1,3] Maike Schumacher[3] Joseph L. Awange ,[1,2,4]

and Hannes Müller Schmied[5,6]

Extreme droughts have profound negative impacts on TWS in the GBM River Basin

Declining TWS in the Brahmaputra-Meghna River Basin likely due to declining rainfall

TWS variations over Ganges and Bangladesh are strongly affected by excessive groundwater withdrawal

Corresponding author: Khandu, Department of Spatial Sciences, Curtin University, Kent Street, Bentley, Western Australia 6102 (khandu@postgrad.curtin.edu.au)

[1]Western Australian Centre for Geodesy

Abstract. Climate extremes such as droughts and intense rainfall events are expected to strongly influence global/regional water resources in addition to the growing demands for freshwater. This study examines the impacts of precipitation extremes and human water usage on total water storage (TWS)

and the Institute for Geoscience Research,
Curtin University, Western Australia,
Australia

[2]Department of Cartographic
Engineering, Universidade Federal de
Pernambuco, Recife, Pernambuco, Brazil

[3]Institute of Geodesy and
Geoinformation, University of Bonn, Bonn,
Germany

[4]Geodetic Institute, Karlsruhe Institute of
Technology, Karlsruhe, Germany

[5]Institute of Physical Geography,
Goethe-University Frankfurt, Frankfurt,
Germany

[6]Biodiversity and Climate Research
Centre (BiK-F) & Senckenberg Research
Institute and Natural History Museum,
Frankfurt, Germany

over the Ganges-Brahmaputra-Meghna (GBM) River Basin in South Asia. Monthly TWS changes derived from GRACE (2002-2014) and soil moisture from three reanalyses (1979-2014) are used to estimate new extreme indices. These indices are applied in conjunction with standardised precipitation indices (SPI) to explore the impacts of precipitation extremes on TWS in the region. The results indicate that although long-term precipitation do not indicate any significant trends over the two sub-basins (Ganges and Brahmaputra-Meghna), there is significant decline in rainfall (9.0±4.0 mm/decade) over the Brahmaputra-Meghna River Basin from 1998-2014. Both river basins exhibit a rapid decline of TWS from 2002-2014 (Ganges: 12.2±3.4 km^3/year and Brahmaputra-Meghna: 9.1±2.7 km^3/year). While the Ganges River Basin has been regaining TWS (5.4±2.2 km^3/year) from 2010 onwards, the Brahmaputra-Meghna River Basin showed a further decline (13.0±3.2 km^3/year) in TWS from 2011 onwards. The impact of human water consumption on TWS appears to be considerably higher in Ganges compared to Brahmaputra-Meghna, where it is mainly concentrated over Bangladesh. The interannual water storage dynamics are found to be strongly associated with meteorological forcing data such as precipitation. In particular, extreme drought conditions, such as those of 2006 and 2009, had profound negative impacts on the TWS, where groundwater resources are already being unsustainably exploited.

1. Introduction

The Ganges-Brahmaputra-Meghna (GBM) River Basin in South Asia, with a drainage area of ∼1.7 million km^2 is the third largest freshwater outlet in the world with a total annual discharge of ∼1,350 km^3 into the Indian Ocean [*Steckler et al.*, 2010]. Its hydrological regime is dominated by the Indian monsoon, which amounts to 60-90% of the annual precipitation. A reasonable area of river basin (22,800 km^2) is covered by glaciers and snowfields, especially over the Himalayan regions of Nepal, Bhutan, southern China and northern India [*Bolch et al.*, 2012]. Although GBM River Basin is endowed with abundant sources of freshwater system, its water resources are becoming increasingly vulnerable due to climate extremes (e.g., droughts) and rapid socio-economic changes (e.g., increasing population and land use changes) [*Rodell et al.*, 2009; *Tiwari et al.*, 2009; *Shamsudduha et al.*, 2009b; *Chen et al.*, 2014; *Central Ground Water Board*, 2014]. Rapid groundwater depletion has been reported across many parts of the GBM River Basin, especially along the vast alluvial plains of Ganges, Brahmaputra, and the delta regions.

Although the Indian monsoon rainfall is projected to increase slowly over the region [see, *Annamalai et al.*, 2007; *Turner and Annamalai*, 2012], current assessments have, however, shown significant decline in rainfall during the past few decades [*Ramanathan et al.*, 2005; *Chung and Ramanathan*, 2006]. This decline has been attributed to increasing emissions of aerosol (sulphate and black carbon) across South Asia [*Ramanathan et al.*, 2005; *Lau et al.*, 2009]. Precipitation extremes and droughts in the context of global warming is of particular concern over the region. Several studies have reported that the GBM River Basin is tending towards a more wetter regime while the number of warm

nights have risen significantly since 1950 [*Klein Tank et al.*, 2006; *Baidya et al.*, 2008]. Droughts have become more frequent over central India, Bangladesh, and Nepal [e.g., *Baidya et al.*, 2008; *Rajeevan and Bhate*, 2008; *Shahid*, 2011] while decreasing heavy rainfall events have been observed over northeast India [e.g., *Roy and Balling*, 2004]. In addition, interannual variation of rainfall over the GBM River Basin is influenced by large-scale ocean-atmospheric interactions such as El Niño Southern Oscillation [ENSO, e.g., *Chowdhury and Ward*, 2004; *Pervez and Henebry*, 2015] and Indian Ocean Dipole [IOD, e.g., *Ashok et al.*, 2001]. Rainfall contributions from ENSO and IOD events further exacerbate climate extremes in the GBM River Basin [see e.g., *Chowdhury and Ward*, 2004; *Pervez and Henebry*, 2015].

Changes in extreme climate events are expected to significantly impact the GBM's water storage, which are already under immense stress due to over exploitation of e.g., groundwater [e.g., *Tiwari et al.*, 2009; *Central Ground Water Board*, 2014; *Döll et al.*, 2014; *Papa et al.*, 2015]. Climate extremes such as delayed/early monsoon, intense rainfall events, prolonged droughts and increased actual evaporation during summer are important factors that are critical to the short-term variations of groundwater resources in the region [*Bollasina et al.*, 2013]. Besides, soil moisture that regulates groundwater recharge, runoff generation, vegetation growth and agricultural process, and evaporation rates [e.g., *Jiménez-Cisneros et al.*, 2014] are more vulnerable to extreme events. Changes in snow, glacier melt, permafrost, as well as rising snowlines in the Himalayas of Nepal, Bhutan, India, and southern China (Tibet), e.g., as a result of global warming affect regional water balance, causing severe water shortages during winter and dry summers [*Bates et al.*, 2008; *Jacob et al.*, 2012].

Despite numerous studies on climate extremes, accurate quantification and attribution of drought and extreme rainfall events is still difficult due to our incomplete understanding of the hydrological process, changing socio-economic patterns, and various definitions used to describe the extremes [e.g., meteorological, hydrological, agricultural, and social droughts, *Dai et al.*, 2004; *IPCC*, 2012]. Extreme indices rainfall/temperature or soil moisture, e.g., Palmer Drought Severity Index (PDSI) [*Dai et al.*, 2004], or standardised indices and thresholds [*Klein Tank et al.*, 2006] are often inadequate in addressing the extent and severity of climate extremes largely due to lack of complete information on the hydrological system. Since the launch of Gravity Recovery and Climate Experiment [GRACE, *Tapley et al.*, 2004] satellite mission in 2002, large-scale variations in total water storage (TWS) changes on a monthly basis can now be realized. As GRACE-derived TWS changes represent integrated changes in all forms of water storage above and underneath the surface of the Earth (sum of groundwater, soil moisture and permafrost, surface water, snow/ice and biomass), it provides a more comprehensive picture of hydro-meteorological extremes and water storage changes in the region.

The GRACE mission has emerged as a valuable tool for monitoring the global (and regional) water resources [*Wouters et al.*, 2014], especially over the GBM River Basin where groundwater abstraction has become a central issue [e.g., *Shamsudduha et al.*, 2009a; *Shum et al.*, 2011; *Central Ground Water Board*, 2014]. Combined estimates from GRACE and hydrological models indicated an average decline of $\sim$17.7 km^3/year [*Rodell et al.*, 2009] between 2002 and 2008 in the Ganges River Basin, 20.4 km^3/year from 2003-2013 over western India [*Chen et al.*, 2014] and a decrease of 54 km^3/year in the GBM River Basin between 2002-2008 [*Tiwari et al.*, 2009]. *Richey et al.* [2015] reported that

the Ganges River Basin shows the largest use of groundwater among the 37 river basins compared. GRACE has demonstrated strong potential for estimating extreme climate events such as floods and droughts [e.g., *Houborg et al.*, 2012; *Long et al.*, 2013; *Thomas et al.*, 2014] and monitoring snow and glaciers [*Matsuo and Heki*, 2010; *Jacob et al.*, 2012].

Given that only few studies have emphasized on the impact of precipitation extremes on the TWS of the region [e.g., *Steckler et al.*, 2010; *Long et al.*, 2014], this study examines the impacts of precipitation extremes (e.g., droughts) and groundwater abstraction on TWS in the GBM River Basin during the past three decades. While a detailed outlook on the impacts of extreme climate events on the basin's TWS may be far from complete due to large uncertainties in observational records and hydrological models, a reasonable effort has been made to address various factors affecting the basin water storage as well as the implications of human water usages based on simulation studies. Particularly, in the present contribution, new extreme indices are generated using observed rainfall datasets, reanalyses-based soil moisture, and GRACE TWS estimates. To address the issue of human water usage, two scenarios simulated by the WaterGAP Global Hydrology Model [WGHM, *Döll et al.*, 2003] for the period 1980-2010 based on the (a) natural water storage variability, and (b) water storage simulated under human water usage are considered.

The remainder of the study is organised as follows. A brief description of the GBM River Basin is provided in Section 2 followed by a summary of various data sets employed in Section 3. The analysis approaches are described in Section 4, and the results discussed in Section 5. The major findings of this study are then summarized in Section 6.

2. Ganges-Brahmaputra-Meghna (GBM) Basin

The GBM River Basin is a transboundary basin shared by 5 countries of India (64%), China (18%), Nepal (9%), Bangladesh (7%) and Bhutan (3%) (Figure 1). Elevation in GBM River Basin ranges from sea level to more than 8,000 m. Ganges and Brahmaputra rivers originate from the snow/ice covered Himalayan mountains in southern China while the Meghna river, also known as Barak, originates from northeast India. All the three rivers meet in Bangladesh before making their way into the Bay of Bengal. The GBM River Basin features distinct climatic characteristics including high topographic variations that significantly impact the spatial rainfall distribution, extratropical disturbances in the north, the Indian monsoon during summer, and teleconnections effects from large-scale ocean-atmospheric interactions [e.g., *Dimri et al.*, 2015]. The winter time precipitation over the northern GBM covering the Himalayas are mainly driven by the mid-latitude sub-tropical jets known as the Western Disturbances, providing additional water mass to the existing glaciers [*Dimri et al.*, 2015].

[FIGURE 1 AROUND HERE.]

The Ganges River Basin is characterised by low precipitation while Brahmaputra and Meghna River Basins are characterised by high rainfall amounts during the monsoon season [*Mirza et al.*, 1998], especially along the Himalayan fronts due to pronounced orographic rainfall [*Barros et al.*, 2004; *Khandu*, 2015]. GBM River Basin receives an average of 1,500 mm/year of annual rainfall [*FAO*, 2011], and is the major source of freshwater used for all socio-economic activities (e.g., drinking, irrigation, agriculture, and hydropower generation). Groundwater is stored in relatively shallow water tables up to 2-10 meters below the ground level in sub-Himalayan regions of Ganges and Brahmaputra

[*Central Ground Water Board*, 2014]. No assessments are available in the mountainous regions of Nepal and Bhutan.

3. Data

The temporal (t) rate of changes in TWS ($\frac{\delta W}{\delta t}$) products are directly related to changes in fluxes, i.e. precipitation (P), evapotranspiration (E), and runoff (R), through the water balance equation: $\frac{\delta W}{\delta t} = P(t) - E(t) - R(t)$. In this study, precipitation is used as the primary meteorological forcing variable to assess the impacts of climate extremes on TWS (and soil moisture) in the GBM River Basin. Soil moisture is an important indicator of agricultural drought. The surface water storage also varies significantly within the GBM River Basin, contributing up to $\sim$ 40-50 % of the TWS variations [*Papa et al.*, 2015]. While the surface water storage variability is already reflected in the extreme indices estimated using GRACE-derived TWS changes, it is not included in the indices estimated from soil moisture data sets. In this study, various products representing precipitation, TWS changes, and soil moisture are used in order to evaluate their spatio-temporal consistency within the region, and to estimate a single solution based on their uncertainties. These products are described as follows:

3.1. Precipitation data

1. **APHRODITE Rain Gauge Data [1979-2007]**: Asian Precipitation Highly Resolved Observational Data Integration Towards Evaluation of Water Resources [APHRODITE, *Yatagai et al.*, 2012] is a Japanese-based international project, which provides daily high resolution ($0.25^\circ \times 0.25^\circ$ and $0.50^\circ \times 0.50^\circ$) gridded rainfall data derived from thousands of rain gauges across Asia from 1951-2007. We use the daily precipitation

estimates (0.50° × 0.50° resolution) from version V1101 (hereafter APHRODITE) covering the period 1979-2007. APHRODITE precipitation data have been shown to agree well with *in-situ* rain gauge records over majority of the GBM River Basin [see, e.g., *Andermann et al.*, 2011; *Khandu*, 2015], and has been applied in various hydrological studies.

2. **TMPAv7 [1998-2014]**: Because APHRODITE was available only up to 2007, the remaining period is complimented by monthly precipitation estimates (TRMM 3B43 version 7) from the Tropical Rainfall Measuring Mission (TRMM) Multi-satellite Precipitation Analysis [TMPA, *Huffman et al.*, 2007] for the period 1998 to 2014, hereafter referred to as TMPAv7. Monthly TMPAv7 precipitation estimates are available at 0.25° × 0.25° spatial resolution and have been further corrected using high-density gauge-based precipitation data sets [see, *Huffman et al.*, 2007].

3. **Other Gauge-based Products**: Monthly gridded precipitation datasets from Global Precipitation Climatology Center [GPCC version 6, *Schneider et al.*, 2014] and Climate Research Unit [CRU TS3.22, *Harris et al.*, 2013] are used to complete our investigations. GPCC version 6 (hereafter GPCCv6) and CRU TS3.22 (hereafter CRU_TS3.22) are applied to assess precipitations from 1979 onwards.

3.2. TWS changes from GRACE [2002-2014]

GRACE is a US/German joint satellite mission that has been continuously monitoring the spatial and temporal variations of the Earth's gravity field since March 2002 [*Tapley et al.*, 2004]. In this study, the latest (RL05) release of GRACE Level 2 products of CSR, GFZ, and JPL (from `ftp://podaac.jpl.nasa.gov/allData/grace/L2/`) covering the period August 2002 to September 2014 are used to estimate TWS changes. The degree one

(C_{10}, C_{11}, S_{10}) and two (C_{20}) components of the spherical harmonics are replaced by those from *Cheng et al.* [2013] and *Cheng and Tapley* [2004], respectively, as these coefficients are not properly estimated. GRACE fields are filtered using the non-isotropic decorrelation filter [DDK2, *Kusche et al.*, 2009] to reduce the north-south stripes. Filtered solutions are then converted to TWS changes following *Wahr et al.* [1998]. Filtering, however, causes some damping of signal amplitude and spatial leakages, which can be restored by introducing a multiplicative scaler (or a gridded) gain factor [e.g., *Landerer and Swenson*, 2012; *Awange et al.*, 2013]. Here, various hydrological models and reanalysis products (see, Section 3.3 and 3.4) are used to compute the gain factor for the two river basins as well as gridded gain factor that is applied to GRACE-derived TWS anomalies. The basin average gain factors obtained for the two river basins are 1.05 for the Ganges and 1.02 for the Brahmaputra-Meghna River Basin.

3.3. TWS changes from WaterGAP [1979-2009]

Monthly time series of TWS outputs of the global water availability and water use model WaterGAP [Water Global Assessment and Prognosis, *Alcamo et al.*, 2003; *Döll et al.*, 2003; *Müller Schmied et al.*, 2014] in its version 2.2a [http://www.uni-frankfurt.de/49903932/7_GWdepletion?, *Döll et al.*, 2014] are used in this study. In the first variant ("NOUSE"), no water use is subtracted, while in the second variant ("IRR70_S") water is subtracted from surface and groundwater with the assumption of deficit irrigation at only 70% of optimal irrigation and groundwater recharge below surface water bodies are calculated in arid regions. Several model variants were investigated in *Döll et al.* [2014] to assess groundwater abstraction and depletion world-wide. Their

findings indicate that "IRR70_S" provides reliable human water use in many regions of the world.

3.4. Soil moisture products [1980-2014]

Skills of several soil moisture products are assessed in order to examine their spatial and temporal consistency over the GBM River Basin. These soil moisture products are described below:.

1. **CPC**: The Climate Prediction Center (CPC) at National Oceanic and Atmospheric Administration (NOAA) generates global monthly soil moisture estimates at $0.5^\circ \times 0.5^\circ$ resolution from 1948-present by forcing their hydrological model using observed precipitation and temperature [*van den Dool et al.*, 2003].

2. **MERRA**: The Modern Era Retrospective Analysis for Research Application [MERRA, *Rienecker et al.*, 2011] reanalysis, is a state-of-art global reanalysis based on an updated modelling and data assimilation system for the satellite-era (1979 onwards) produced by the National Aeronautic and Space Administration (NASA, US). MERRA reanalysis integrates various observational datasets from modern observing systems such as satellite-based estimates [*Rienecker et al.*, 2011] to describe various conditions of the meteorological and hydrological process including soil moisture, snow/ice, canopy water, among others. The retrospective-analyses is run globally at a relatively high spatial resolution ($0.67^\circ \times 0.50^\circ$) at 6-hourly time intervals. In this study, monthly root-zone soil water contents or soil moisture data are considered (see, `http://gmao.gsfc.nasa.gov/merra/`).

3. **ERA-Interim**: ERA-Interim is a global atmospheric reanalysis produced by the European Center for Medium Range Weather forecast [ECMWF, *Dee et al.*, 2011]. The reanalysis delivers several key land surface parameters such as soil moisture, vegetation,

and snow, among others by combining various global observational datasets using a integrated forecast model. In this study, monthly soil moisture data from four volumetric layers are obtained from 6-hourly $0.75^\circ \times 0.75^\circ$ soil moisture data, which are available at `http://apps.ecmwf.int/datasets/data/interim-full-daily/`.

4. **GLDAS**: The Global Land Data Assimilation System (GLDAS) is a land surface model developed by *Rodell et al.* [2004] with advanced land surface modeling and data assimilation techniques, and are designed to generate optimal fields of land surface states and fluxes through assimilation of huge quantity of ground-based and SRS-based observational products [*Rodell et al.*, 2004]. GLDAS drives several models including Noah, Mosaic, VIC, and Community Land Model (CLM) [see, *Rodell et al.*, 2004, and references therein], with variable soil layers and depth columns, and are run at a $0.25^\circ \times 0.25^\circ$ horizontal resolution. Previous studies have used GLDAS fields to derive groundwater storages from GRACE-derived TWS fields over various parts of the GBM River Basin [e.g., *Rodell et al.*, 2009; *Tiwari et al.*, 2009; *Shamsudduha et al.*, 2009b]. Here, three GLDAS models including Noah, Mosaic, and VIC, are used to estimate soil moisture variability over the GBM River Basin.

The comparison results of various soil moisture products are given in the Supporting Information. Soil moisture data sets vary considerably between the different products. The annual amplitudes are the largest (smallest) in CPC, Noah, and Mosaic (ERA-Interim) (see, Figure S1). However, soil moisture data sets from three GLDAS land surface models are found to contain spurious jumps between 1995 and 1997 (see, Figure S3). Soil moisture variability from WGHM appears to be substantially lower than those shown by the others products due to its relatively low available soil water capacity (around 100

mm in the study regions). Since soil moisture of WGHM can range only between wilting point and field capacity [*Müller Schmied et al.*, 2014], it tends to limit the overall seasonal and interannual variation (see, Figures S2 and S4). These products were therefore, not considered for further analysis in this study.

4. Methods

4.1. Extreme indices

All the data sets are converted to a common grid resolution of $0.5° \times 0.5°$. To investigate the influence of precipitation extremes on TWS changes, the following two extreme indices that describe the severity and duration of extremes were considered.

1. **Standardised Precipitation Index (SPI)**: SPI is a widely used measure of meteorological drought to monitor rainfall deficits based on probability distribution of long-term precipitation time series [e.g., *McKee et al.*, 1993; *Hirschi et al.*, 2011]. To determine periods of medium to long-term scales of precipitation extremes, here, SPI is estimated by fitting a two-parameter γ-distribution to 6-month running mean precipitation time series. As in *McKee et al.* [1993] and *Hirschi et al.* [2011], SPI values greater than ± 2.0 are considered as extremes while values between ± 1.5 to ± 2.0 are assumed as moderate extreme events (see details in Table 1).

2. **Standardised Index (SI)**: SI is developed based on TWS and soil moisture time series to provide relevant classification of hydrological droughts in the region as well as to determine their periods with respect to meteorological droughts (derived from SPI). In order to compute SI, temporal anomalies of TWS and soil moisture are derived by removing the linear trends, annual, and semi-annual amplitudes from the individual time

series using a multiple linear regression model:

$$\mathbf{X} = x(t,j) = \beta_1(j).t + \beta_2(j).cos(2\pi t) + \beta_3.(j)sin(2\pi t) + \beta_4(j).cos(4\pi t) + \beta_5(j).sin(4\pi t) + \epsilon(t), \quad (1)$$

where $\mathbf{X}$ contains the temporally centered value of interest (e.g., TWS) at time t and position j, β_1 to β_5 are regression coefficients corresponding to linear trend (β_1), annual (β_2 and β_3), and semi-annual (β_4 and β_5) cycles, and ϵ represents the random error terms. The residual signal ($\hat{\mathbf{X}}_e$) is derived by removing the dominant terms (linear trend, annual, and semi-annual cycles) as:

$$\hat{\mathbf{X}}_e = \hat{x}_e(t,j) = x(t,j) - \left(\hat{\beta}_1(j).t + \hat{\beta}_2(j).cos(2\pi t) + \hat{\beta}_3.(j)sin(2\pi t) + \hat{\beta}_4(j).cos(4\pi t) + \hat{\beta}_5(j).sin(4\pi t)\right), \quad (2)$$

where $\hat{\beta}_1$ to $\hat{\beta}_5$ are estimated coefficients derived by fitting Equation 1 to the time series using a least squares adjustment approach. The residuals ($\hat{\mathbf{X}}_e$) in Equation 2 contain information on the temporal variation in extremes. The SI values are then obtained by dividing by their respective standard deviations over a running mean of 6 months. The obtained SI time series are given in Table 1.

[TABLE 1 AROUND HERE.]

4.2. Correlation and trend analysis

Long-term (or decadal, in case of GRACE data sets) trends in precipitation and TWS (using Equation 1) are analysed to assess the impact of precipitation changes on the basin's water storage from 1979-2014 (and 2002-2014). The significance of the linear trends are tested at 95% confidence level using the non-parametric Mann-Kendall's test [*Mann*, 1945; *Kendall*, 1962] after removing the dominant annual and semi-annual terms

(see, e.g., Equation 2). In addition, a cross correlation analysis is carried out between precipitation and TWS (and/or soil moisture) to examine the relationship between meteorological forcing data (e.g., precipitation) and TWS over the GBM River Basin.

4.3. Error estimation of various datasets

A modified three-cornered-hat (TCH) method is applied to estimate relative uncertainties in each of the hydrological products. The uncertainty estimates are then used as a basis to compute weighted averages of rainfall, soil moisture, and TWS changes for analyzing hydrological extremes. Our motivation to use TCH for error estimation is that unlike conventional approaches, TCH does not require true reference fields. This is particularly useful here since true estimates of such fields are not easily obtainable (e.g., TWS). The TCH method is formulated here following *Awange et al.* [2015] that accounts for correlated errors resulting from the use of same observational sources such as in merged remote-sensing products or reanalysis products. Applying TCH approach, however, requires at least three datasets to estimate uncertainties. Therefore, all products described in Section 3 are considered. To represent the strength of signal in each product against existing background noise, signal-to-noise ratio (SNR) is estimated based on the derived uncertainty estimates.

5. Results and Discussion

5.1. Trends in rainfall and water storage changes

This section presents the long-term and decadal trends of the individual hydrological variables in the GBM River Basin from 1979-2014 where Figures 2a-c show the spatial distribution of rainfall trends based on APHRODITE, GPCCv6, and CRU_TS3.22 products.

During this period, no significant changes are found between 1979 and 2007 except for a few grid cells located in Ganges River Basin that indicate negative trends. From 1998-2014 (TMPAv7), however, significant decline is found in rainfall, especially over northern Bangladesh and Nepal, western Bhutan, and parts of northeast India (Figure 2e). The gauge-only CRU_TS3.22 dataset also indicates the decreasing rainfall trend over northern Bangladesh consistent with those of TMPAv7. It has been suggested that declining rainfall patterns found over the region were likely due to severe droughts across the GBM River Basin from early 2000 onwards [*Miyan*, 2014]. On the other hand, Figures 2d-e also indicate significant increasing rainfall amounts over the western Ganges basin from 1998 onwards. Basin-averaged precipitation time-series (figure not shown) also indicate no significant changes during 1979-2007 in both basins. From 1998-2014, however, a significant decline is found in monthly rainfall amount (9.0±4.0 mm/decade) over the Brahmaputra-Meghna River Basin based on TMPAv7. CRU_TS3.22 data shows a decline of 6.0±3.8 mm/decade for the 1998-2013 period over the same river basin while no significant changes are detected in the Ganges River Basin.

[FIGURE 2 AROUND HERE.]

Figure 3 shows the linear trends of soil moisture over the GBM River Basin based on three global reanalysis products. MERRA and CPC indicate similar patterns of increase in soil moisture over the Himalayan foothills (Figures 3a and 3c) while ERA-Interim shows increasing trends mainly over the western parts of GBM. Considering CPC results, the largest increasing trend is found being at a rate of >40 mm/year, mainly distributed over the Himalayan region. Unlike the other two products, MERRA shows large decreasing trends over the Southeast Asian region. Given the level of uncertainty among these three

reanalyses (see also, Supporting Information), it is difficult to characterize their long-term trend in the GBM River Basin. Moreover, *Mishra et al.* [2014b] reported that soil moisture in the Ganges River Basin has declined substantially during autumn between 1950 and 2005 following a significant decline in rainfall during the same period.

[FIGURE 3 AROUND HERE.]

Figure 4 shows TWS changes (from GRACE) over a spatial domain that includes the GBM River Basin from August 2002 to December 2014. Linear trends of TWS from all three GRACE products (i.e., CSR, GFZ, and JPL) indicate widespread decline in water storage over the GBM with the largest decline (of $\sim$ 30 mm/year) over Punjab and Haryana [see also, *Chen et al.*, 2014]. The results also indicate that Brahmaputra-Meghna River Basin experienced significant decline in TWS (10-25 mm/year), which might be (partly) due to decrease in rainfall (see, Figure 2d-e). Nevertheless, it is important to note that groundwater abstraction could still be a significant contributor of TWS decline. Note that evaluation of groundwater storage is not carried out in this study due to lack of access to groundwater data. Groundwater depletion (contributing to TWS decline) across Bangladesh was recently reported by *Döll et al.* [2014], who used WGHM forced by observed meteorological data [see also, *Shamsudduha et al.*, 2009b].

[FIGURE 4 AROUND HERE.]

In terms of the surface water storage, *Papa et al.* [2015] reported that monthly surface water storage variations contributed to about 45% of TWS changes within GBM River Basin from 2003-2007. Here, surface water storage changes are analyzed based on those simulated by WGHM. Estimated linear trends are shown in Figure 5, which shows a decrease of up to $\sim$ 10 mm/year from 1979-2009 (Figure 5a). Consistent with the results

of *Papa et al.* [2015], declining trends (up to $\sim$ 30 mm/year) are found in the south of Meghna and northwest of Brahmaputra River Basins over the period 1979 to 2009. In general, surface water storage appears to be increasing over the Ganges River Basin (see, Figure 5b).

[**FIGURE 5 AROUND HERE.**]

Overall, there is a significant decline in TWS, which is decreasing at the rate of 12.2$\pm$3.4 km^3/year and 9.1$\pm$2.7 km^3/year in the Ganges and Brahmaputra-Meghna River Basins, respectively. Over the extended drought period (2002-2010), Ganges River Basin shows a declining rate of 19.3$\pm$3.9 km^3/year (Figure 6a) while TWS is decreasing at the rate of 7.8$\pm$2.1 km^3/year in the Brahmaputra-Meghna River Basin (Figure 6b). Noticeably, an increasing trend (5.4$\pm$2.2 km^3/year) is seen in the Ganges River Basin after 2010 (Figure 6a). This could have resulted from the recent increase in rainfall following several events of weak to strong La Niña activities from 2010 onwards. However, a rapid decline in TWS (13.0$\pm$3.2 km^3/year) has occurred in the Brahmaputra-Meghna River Basin since 2011 (Figure 6b), which could be attributed to the weak rainfall after 2009.

[**FIGURE 6 AROUND HERE.**]

Uncertainties in precipitation, soil moisture, and TWS are calculated using the modified generalized TCH algorithm as described in Section 4.3. Table 2 summarizes the basin-averaged uncertainty magnitudes of monthly precipitation estimates for the common data period of 1998-2007, soil moisture (1979-2014), and GRACE TWS changes (2002-2014). Among the four precipitation products analysed, APHRODITE tend to show the largest uncertainty ($\sim$30 mm/month) over the Brahmaputra-Meghna River Basin. APHRODITE as well as CRU_TS322 also show considerably higher uncertainty in the

Ganges River Basin. GPCCv6 and TMPAv7 products show very similar skills (with relatively smaller magnitudes of error) in both river basins. Consistent with the TCH results, both APHRODITE and CRU_TS322 indicate relatively lower monsoon rainfall amount over the 10-year period (results not shown).

Among the soil moisture products, Figure 3 already showed that the three products (MERRA, ERA-Interim, and CPC) do not agree very well on the long-term trends with CPC showing anomalously large increases in the region. In terms of interannual variability, ERA-Interim shows the largest uncertainty with an average magnitude of ∼44 mm/month over the GBM River Basin. MERRA appears to be more reliable with an error magnitude of ∼10 mm/month. Uncertainties are expressed in terms of SNR by dividing their respective root-mean-squares (RMS) by their uncertainty estimates derived from the TCH method. All three reanalyses show very similar spatial patterns of SNR but with varying magnitudes (Figure 7). ERA-Interim shows the least SNR values, which are consistent with error magnitudes shown in Table 2. Among the GRACE products, TWS changes derived from CSR shows the lowest uncertainty (∼5 mm/month) (see, Table 2).

[FIGURE 7 AROUND HERE.]

[TABLE 2 AROUND HERE.]

Figure 8 shows correlation coefficients between monthly rainfall, soil moisture, and GRACE TWS changes for the period 2002-2014. Correlations between precipitation and GRACE TWS are high (>0.6) and significant (at 95% confidence level) over majority of the GBM River Basin with a time-lag of 1-2 months (Figure 8a-b). There is also very high correlation between soil moisture and TWS (Figure 8c-d) with a time-lag of up to one month. Correlations between rainfall and soil moisture (in Figure 8e) are considerably

larger than those between rainfall and TWS, with a similar time-lag (of 1-2 months). The lag relationship between various variables represents the surface hydrological process in the region, and are particularly significant considering the high correlation values within the GBM River Basin. The low correlation coefficients seen in the mountain regions of northwestern Nepal and the Karakorum region in the Hindu Kush mountains (i.e., outside the study region) can also be explained by the poor accuracy (or ungauged) of observed precipitation data [e.g., *Khandu*, 2015]. These low (or negative) correlations may also indicate the mismatch in seasonality between rainfall and TWS variability or limited influence of precipitation over the region.

[**FIGURE 8 AROUND HERE.**]

5.2. Evidences of climate extremes

Meteorological droughts are caused by climate fluctuations over extended period of time, resulting from non-availability of or below normal rainfall. Meteorological droughts may then lead to other problems such as decreasing or drying surface water or depletion of groundwater (hydrological drought), and depletion of soil moisture (agricultural drought) [*Dai et al.*, 2004]. Extreme precipitation events may either relieve water stress through increased recharge rates or aggravate water-stress through soil erosion, increased runoffs, and floods [*Taylor et al.*, 2013]. Besides climatic influences, the GBM River Basin has experienced significant reduction in water storage due to increased surface water and groundwater abstraction [e.g., *Tiwari et al.*, 2009; *Central Ground Water Board*, 2014; *Papa et al.*, 2015], with further contributions from fast shrinking glaciers in the Himalayas [e.g., *Scherler et al.*, 2011; *Bajracharya et al.*, 2015]. Thus, both effects should be accounted for when analysing the interannual variations of TWS. This section investi-

gates the possible influences of precipitation extremes on the variability of soil moisture and TWS in the GBM River Basin based on indices that are estimated from each of the data sets.

Figure 9 shows the interannual variability of monthly rainfall, soil moisture, and TWS. All three variables shows considerable interannual variability. Soil moisture and TWS shows a delayed response from the driving meteorological forcing rainfall. The major peaks seen in Figure 9 mostly reflect low frequency variations of ENSO, indicating the dominant effects of large-scale climate variations. Further, it is observed that prolonged drought conditions likely exacerbated TWS in the Ganges River Basin (Figure 9a) whereas extreme rainfall events tend to favour TWS in Brahmaputra-Meghna River Basin (Figure 9). This indicates that water storage changes in Ganges River Basin are likely to be more vulnerable to meteorological droughts.

[**FIGURE 9 AROUND HERE.**]

A more quantitative estimate can be obtained by plotting the cumulative sums of each of the variables as shown in Figure 10. While the rainfall have remained below average since the mid of 2005 in the Ganges River Basin with a decline of up to 400 mm in 2010, the TWS has shown an unprecedented decline from 2009-2011 with a decrease of about 1,200 mm in ∼29 months (Figure 10a). For the same period, accumulated soil moisture decreased by about 600 mm before returning to the normal level by the start of 2014. In the Brahmaputra-Meghna River Basin, changes are relatively smaller except between 2005 and 2007 when accumulated TWS decreases by about 400 mm, but it returned to the same level by the start of 2009. The differences between TWS and soil moisture curves are partly due to the strong variability of surface water over GBM that is reflected

in GRACE observations but is missing in reanalysis. From Figure 10, it is observed that the magnitude of TWS changes is larger than precipitation (e.g., in 2009), which indicates the combined effect of meteorological drought and human water abstraction in the two basins. Such unprecedented decrease of TWS in the Ganges River Basin during the drought period of 2009-2010 has not been previously reported [e.g., *Central Ground Water Board*, 2014; *Richey et al.*, 2015].

[**FIGURE 10 AROUND HERE.**]

Climate extremes are more often described by statistical indices for practical applications (e.g., climate impact analysis, engineering designs). To categorize various extreme events, SPI (derived from precipitation), and SI of soil moisture and TWS changes are plotted in Figure 11. Both river basins experienced more frequent meteorological droughts than extreme rainfall events between 1979 and 2014. Severe drought events over the Ganges River Basin (SPI < -1.5) include: 1991-1994, 2001-2003, 2005-2007, and 2009-2010 (Figure 11a), while those of the Brahmaputra-Meghna River Basin include: 1981-1983, 1986, 1992-1994, 1999, 2005-2006, and 2009-2010 (Figure 11b). Extreme rainfall events (SPI < -2.0) and prolonged droughts from 1991-1994 led to the longest (50 months) hydrological drought (i.e., soil moisture deficit) in the Ganges River Basin (Figure 11a).

SI from GRACE TWS changes shows extreme droughts (SI < -2.0) from 2009-2010 in the Ganges River Basin (Figure 11a) and from 2005-2007 and 2009-2010 in the Brahmaputra-Meghna River Basin (Figure 11b), with a lag of about 4-6 months. These results are consistent with the SPI and soil moisture indicating that simulated soil moisture products responds quite well to the meteorological droughts. A summary of recent

drought events (from 2002-2014) including their duration and intensity are provided in Table 4. Moderate to extreme rainfall events (SPI $>$ 1.5) are dominant during 1980-1990, 1997-1999, and 2010-2013 over the Ganges River Basin, while the Brahmaputra-Meghna River Basin experiences extreme rainfall events during 1982-1990, 1998, and in 2004, 2007, and 2010. These extreme rainfall events restore soil moisture deficits in most of the occasions except that of 1983 in the Brahmaputra-Meghna River Basin (Figure 11b).

[FIGURE 11 AROUND HERE.]

Temporal correlation coefficients are calculated over the common data period of 2002-2014 between SPI and SI of TWS (and soil moisture) to quantify their relationships (see, Table 3). Correlations between SPI and SI of TWS are found to be significant with a value of 0.6 and 0.4 for the Ganges and Brahmaputra-Meghna River Basins, respectively. The correlation values between SPI and SI of soil moisture are 0.8 and 0.6 for the two basins with a time lag of 2-4 months (Table 3). The lower correlation values observed between SPI and SI of TWS can be explained by the below normal rainfalls after 2011 (see, Figure 11). It is also worth mentioning here that correlations between rainfall and TWS do not take into account the complex hydrological fluxes in the Himalayas, where dynamics of snow/ice plays a much bigger role. The relationship between soil moisture and TWS is, however, considerably higher with a correlation of 0.7-0.8, in both basins. Thus, simulated outputs from three reanalysis adequately captures the extreme patterns within GBM River Basin.

[TABLE 3 AROUND HERE.]

[TABLE 4 AROUND HERE.]

Rainfall variability of June-September (corresponding to the Indian monsoon rainfall) over 1980-2014 shown in Figure 12a indicates strong interannual variations along with a declining trend after 1998. This might support the findings of [*Chung and Ramanathan*, 2006] who reported that monsoon circulation has been weakening over the few decades accompanied by decreasing heavy rainfall events over northeast India [see also, *Roy and Balling*, 2004; *Goswami et al.*, 2010]. For the winter precipitation, recent reports have suggested an increase in rainfall amount over the years due to enhanced activities of the westerlies [*Scherler et al.*, 2011; *Bajracharya et al.*, 2015]. However, between 1980 and 2014, our results indicate an overall decrease in winter precipitation at 7.0±3.0 mm/decade in the Brahmaputra-Meghna River Basin (Figure 12b). Based on this findings, it is clear that climate variability plays a significant role on the reduction of stored water in the GBM River Basin.

[**FIGURE 12 AROUND HERE.**]

Next, we examine hydrological extremes and their relationship to ENSO and IOD events. Heavy rainfall events generally occur during La Niña (represented by negative values of the ENSO index, Niño3.4, `http://www.cpc.ncep.noaa.gov/products/analysis_monitoring/ensostuff/ensoyears.shtml`) periods while drought conditions were found to occur mostly during El Niño (represented by positive values of Niño3.4) conditions [e.g., *Ashok and Saji*, 2007; *Pervez and Henebry*, 2015]. For example, the extreme rainfall events of 1984, 1987-1988, 1998, and 2011 in the Ganges River Basin occurred during the periods of major La Niña events and has shown similar occurrences of extremes in the Brahmaputra-Meghna River Basin (see, Figure 11). Similarly, major droughts during the years 1982, 1987, 1991-1995, 2002, and 2009 in the Ganges River Basin and 1982-1983,

1991-1992, 1994, 2005, and 2009 in the Brahmaputra-Meghna River Basin occurred during weak-to-very strong El Niño conditions. The 2009-2010 strong El Niño event led to the single largest drought episode in the region in the past three decades with monsoon rainfall falling below 50 mm/month (Figure 12a). This drastic decline in rainfall led to a sharp decline in TWS (about 1200 mm within a period of about 29 months) in the Ganges River Basin (see, Figure 10a). However, not all extremes occur during ENSO events and an opposite relationship can be found in some years (e.g., in 1983-1984 and 1997-1998).

The IOD [*Saji et al.*, 1999], which is commonly measured by the Dipole Mode Index (DMI, see, `http://www.jamstec.go.jp/frcgc/research/d1/iod/iod/dipole_mode_index.html`) also has strong influence on the Indian monsoon variability [see e.g., *Ashok and Saji*, 2007], and hence are associated with hydro-meteorological extremes over the GBM River Basin. For instance, strong positive IOD events in 1983-1984 and 1997-1998 were associated with extreme rainfall events in the Ganges River Basin (Figure 10) with both occurring under strong prevailing El Niño conditions. Overall, the relationship between ENSO/IOD and extreme indices of rainfall (or TWS) were found to be insignificant over period 2002-2014 (results not shown).

5.3. Impact of human water abstraction on TWS

To assess the anthropogenic impacts on the basin water usage during the past 3 decades, simulated TWS outputs of WGHM from two different scenarios (see details Section 3.3) are analyzed. The root-mean-square (RMS) of the difference in monthly TWS between "NOUSE" and "IRR70_S" is determined to quantify the impact of human water usage for each individual grid cell over the period 1979-2009 (Figure 13). Based on Figure 13, a rather small influence of human water abstraction is found over the Brahmaputra-Meghna

River Basin, i.e. RMS values of < 2 mm in more than 96% of the basin. However, large values of up to 13 cm are obtained over northern and central Bangladesh, where high activities of groundwater abstraction have been reported [see e.g., *Shamsudduha et al.*, 2009a; *Shamsudduha*, 2013]. In the Ganges River Basin, RMS values larger than 10 cm are obtained in approximately 23% of the basin, with differences exceeding more than 1 m in 3% of the grid cells, especially in the western part (see, Figure 13). The simulation results are consistent with those released by the Indian government on the use of groundwater resources [e.g., *Central Ground Water Board*, 2014] and the TWS trends shown in Figures 4 and 6.

[FIGURE 13 AROUND HERE.]

Figure 14 compares the basin-averaged time series of "NOUSE" and "IRR70_S" simulations between 1979 and 2009 for the Ganges River Basin. In order to directly compare the TWS variation and to see the development in time including and excluding human water use, the off-set between the two curves is removed by subtracting the TWS values of January 1979 from both curves. The difference between the two curves increases with time, showing a clear impact of human activities on TWS changes in Ganges. The linear trend of the difference over 1979-2009 is -14 mm/year (or 15 km^3/year). While the trend of 1979-2001 is -12 mm/year (or 13 km^3/year), it increased to -20 mm/year (or 22 km^3/year) during 2002-2009. The latter estimate agrees well with the trend of GRACE TWS for the same period (see, Figure 6) and those reported in *Tiwari et al.* [2009] and *Richey et al.* [2015]. The increasing level of groundwater abstraction in the Ganges River Basin was also reported in a global-wide basin study in *Richey et al.* [2015]. Besides the impact of human water abstraction, several studies indicate that Himalayan glaciers are

retreating due to climate change [*Scherler et al.*, 2011; *Bajracharya et al.*, 2015], which could also contribute to the overall decline of TWS over both the sub-basins through increased runoffs during the spring season (March-May).

[**FIGURE 14 AROUND HERE.**]

6. Summary and Conclusion

The Ganges-Brahmaputra-Meghna (GBM) River Basin in South Asia is highly vulnerable to extreme hydrological events such as heavy rainfall, prolonged droughts, flooding, and glacial lake outburst floods [e.g., *Mirza et al.*, 1998; *Bates et al.*, 2008; *Jiménez-Cisneros et al.*, 2014; *Pervez and Henebry*, 2015]. Intensification of one or more of these extremes are likely to exacerbate the rapidly declining rate of TWS [e.g., *Tiwari et al.*, 2009; *Shamsudduha et al.*, 2009b; *Central Ground Water Board*, 2014] in the region. In this study, a suite of observed rainfall, reanalysis-based soil moisture, and GRACE total water storage (TWS) changes, along with hydrological model simulations are applied to examine the impacts of climate extremes and human influences on the GBM's water storage over varying time periods between 1979 and 2014. While the driving precipitation has been relatively stable over the past three decades (1979-2007) in both basins (Ganges and Brahmaputra-Meghna), there has been a significant decline in rainfall over the Brahmaputra-Meghna River Basin from 1998 onwards. The basin-averaged monthly rainfall shows a decline of 9.0±4.0 mm/decade with substantial decline in winter (December-February) rainfall of 7.0±3.0 mm/decade between 1998 and 2014.

Consistent with the previous studies [*Rodell et al.*, 2009; *Tiwari et al.*, 2009; *Richey et al.*, 2015], GRACE TWS changes indicate a rapid decline in TWS (mainly resulting from groundwater) with a rate of 12.2±3.4 km^3/year and 9.1±2.7 km^3/year in the

Ganges and Brahmaputra-Megna River Basin, respectively from 2002-2014. Further analysis shows a decreasing rate of $\sim$19.3$\pm$3.9 km^3/year between 2002-2010 but has increased (at a rate of 5.4$\pm$2.2 km^3/year) from 2010 onwards resulting in an overall smaller TWS decline in the Ganges River Basin. The Brahmaputra-Meghna River Basin, on the other hand, has experienced a drastic decline (at a rate of 13.0$\pm$3.2 km^3/year) of TWS since 2011. An overall decreasing rainfall between 1998 and 2014 (especially over Bangladesh and northeast India) accompanied by anomalously low rainfall from 2012 may have lead to a larger TWS decline in the Brahmaputra-Meghna River Basin. However, trends in soil moisture products are found to be highly inconsistent among the various reanalysis products although they tend to capture seasonal patterns reasonably well over the two basins. Given the level of socio-economic activities in the region, such drastic declines in TWS may also be aggravated by continued withdrawal of groundwater for irrigation during the prolonged drought periods. To address the growing human water usage in the region, simulated outputs from WaterGAP Global Hydrology Model (WGHM) are used. From 1979-2009, intense groundwater abstraction is seen especially in the western Ganges River Basin, reaching up to 1.3 m/year in some regions. The annual rate of groundwater (and/or surface water) abstraction in the Ganges River Basin is estimated at 22 km^3 during the period 2002-2009.

The basin-averaged time series of TWS changes (and soil moisture) derived from GRACE measurements (and reanalyses products), after removing their long-term trends, contain strong seasonal and interannual dynamics in response to meteorological forcing, in particular precipitation extremes. Significant correlations are found between precipitation extremes and TWS/soil moisture (based on their respective indices). The correlation

coefficients range from 0.4-0.6 (for TWS) and 0.6-0.8 (for soil moisture) with a phase lag of 2-4 months. The multiple integrative composition of GRACE TWS reflects changes in all storage components (of the hydrological system) including pronounced effects from continuous groundwater withdrawals during drought periods and melting snow/glaciers in the Himalayas. Thus, correlations between rainfall and TWS only reflect the level of meteorological forcing on the identified extreme events.

Prolonged meteorological droughts are observed to have a major influence on the TWS decline as indicated by the recent drought episodes of 2005-2006 and 2009-2010. Between 2009 and 2011, a TWS declined by about 1,200 mm over a period of 29 months in the Ganges River Basin. Similarly, a decline of about 500 mm was observed between 2005 and 2007 in the Brahmaputra-Meghna River Basin. The interannual variability of the water storage in the GBM River Basin is also found to be moderately influenced by large-scale ocean-atmosphere phenomena such as ENSO and IOD due to their influence on the Indian monsoon.

Acknowledgments. The authors are very grateful to the Editors, Prof. A. Montanari and Prof. B. Scanlon, and anonymous reviewers for their comments, which helped to improve the quality of this manuscript. Khandu is grateful to Curtin Strategic International Research Scholarship, Curtin University (Australia) for the financial support. He also acknowledges the financial support of Prince Albert II of Monaco Foundation and the Intergovernmental Panel on Climate Change (IPCC). E. Forootan acknowledges the research grant provided by the Western Australian School of Mines (WASM)/TIGeR, Curtin University (Australia). J. Awange appreciates the financial support from Alexan-

624 der von Humboldt that supported his stay in Karlsruhe Institute of Technology (KIT),
625 Germany. Khandu and J. Awange also acknowledges the financial support from Brazilian
626 Science Without Borders Program/CAPES Grant No. 88881.068057/2014-01 in collabo-
627 ration with the Federal University of Pernambuco (UFPE, Brazil). Further, the authors
628 are grateful to APHRODITE, Climate Research Unit (CRU), Global Precipitation Clima-
629 tology Centre (GPCC), National Aeronautics and Space Administration (NASA), Center
630 for Space Research (CSR), GeoForschungsZentrum (GFZ), Jet Propulsion Laboratory
631 (JPL), the Climate Prediction Center (CPC), and the European Centre for Medium-
632 Range Weather Forecasts (ECMWF) for providing the necessary data sets used in this
633 study.

References

Alcamo, J., P. Döll, T. Henrichs, F. Kaspar, B. Lehner, T. Rösch, and S. Siebert (2003), Development and testing of the WaterGAP 2 global model of water use and availability, *Hydrol. Sci. J.*, *48*(3), 317–337, doi:10.1623/hysj.48.3.317.45290.

Andermann, C., S. Bonnet, and R. Gloaguen (2011), Evaluation of precipitation data sets along the Himalayan front, *Geochem. Geophys.*, *7*(12), doi:10.1029/2011GC003513.

Annamalai, H., K. Hamilton, and K. R. Sperber (2007), The South Asian Summer Monsoon and its relationship with ENSO in the IPCC AR4 Simulations, *J. Clim.*, *20*(6), 1071–1092, doi:10.1175/JCLI4035.1.

Ashok, K., and N. H. Saji (2007), On the impacts of ENSO and Indian Ocean dipole events on sub-regional Indian summer monsoon rainfall, *Nat. Hazards*, *42*(2), 273–285, doi:10.1007/s11069-006-9091-0.

Ashok, K., Z. Guan, , and T. Yamagata (2001), Impact of the Indian Ocean dipole on the relationship between the Indian monsoon rainfall and ENSO, *Geophys. Res. Lett.*, *28*(23), 4499–4502, doi:10.1029/2001GL013294.

Awange, J., V. Ferreira, Khandu, S. Andam-Akorful, E. Forootan, N. Agutu, and X. He (2015), Uncertainties in remotely-sensed precipitation data over Africa, *Int. J. Climatol.*, *36*(1), doi:10.1002/joc.4346.

Awange, J. L., R. Anyah, N. Agola, E. Forootan, and P. Omondi (2013), Potential impacts of climate and environmental change on the stored water of Lake Victoria Basin and economic implications, *Water Resour. Res.*, *49*, 1–15, doi:10.1002/2013WR014350.

Baidya, S., M. L. Shrestha, and M. M. Sheikh (2008), Trends in daily climatic extremes of temperature and precipitation in Nepal, *Soc. Hydro. and Meteor. (Nepal)*, *5*, 37–51.

Bajracharya, S. R., S. B. Maharjan, F. Shrestha, W. Guo, S. Liu, W. Immerzeel, and B. Shrestha (2015), The glaciers of the Hindu Kush Himalayas: current status and observed changes from the 1980s to 2010, *Int. J. Water Resour. Dev.*, *13*(2), 161–173, doi:10.1080/07900627.2015.1005731.

Barros, A. P., G. Kim, E. Williams, and S. W. Nesbitt (2004), Probing orographic controls in the himalayas during the monsoon using satellite imagery, *Nat. Hazards Earth Syst. Sci.*, *4*(1), 29–51, doi:10.5194/nhess-4-29-2004.

Bates, B., Z. W. Kundzewicz, S. Wu, and J. Palutikof (2008), Climate change and water, in *IPCC Technical Paper VI*, p. 210 pp., Intergovernmental Panel on Climate Change (IPCC), IPCC Secretariat, Geneva.

Bolch, T., A. Kulkarni, A. Kääb, C. Huggel, F. Paul, J. G. Cogley, H. Frey, J. S. Kargel, K. Fujita, M. Scheel, S. Bajracharya, and M. Stoffel (2012), The state and fate of Himalayan glaciers, *Science*, *336*, 310–314, doi:10.1126/science.1215828.

Bollasina, M. A., Y. Ming, and V. Ramaswamy (2013), Earlier onset of the Indian monsoon in the late twentieth century: The role of anthropogenic aerosols, *Geophys. Res. Lett.*, *40*(14), 3715–3720, doi:10.1002/grl.50719.

Central Ground Water Board (2014), Dynamic ground water resources of india (*as on 31st March 2011*, *Tech. Rep. 122*, Ministry of Water Resources, River Development and Ganga Rejuvenation, Government of India, Faridabad, India.

Chen, J., J. Li, Z. Zhang, and S. Ni (2014), Long-term groundwater variations in Northwest India from satellite gravity measurements, *Glob. Planet. Chang.*, *116*, 130–138, doi:10.1016/j.gloplacha.2014.02.007.

Cheng, M. K., and B. D. Tapley (2004), Variations in the earth's oblateness during the past 28 years, *Geophys. Res. Lett.*, *109*(B9), doi:10.1029/2004JB003028.

Cheng, M. K., J. C. Ries, and B. D. Tapley (2013), Geocenter variations from analysis of slr data, in *Reference Frames for Applications in Geosciences*, *International Association of Geodesy Symposia*, vol. 138, pp. 19–25, Springer Berlin Heidelberg.

Chowdhury, M. D. R., and N. Ward (2004), Hydro-meteorological variability in the greater Ganges-Brahmaputra-Meghna basins, *Int. J. Climatol.*, *24*(12), 1495–1508, doi:10.1002/joc.1076.

Chung, C. E., and V. Ramanathan (2006), Weakening of North Indian SST gradients and the monsoon rainfall in India and the Sahel, *J. Clim.*, *19*, 2036–2045, doi:10.1175/JCLI3820.1.

Dai, A., K. E. Trenberth, and T. Qian (2004), A global data set of Palmer Drought Severity Index for 1870-2002: Relationship with soil moisture and effects of surface warming, *J. Hydrometeorol.*, *5*, 1117–1130, doi:10.1175/JHM-386.1.

Dee, D. P., S. M. Uppala, A. J. Simmons, P. Berrisford, P. Poli, S. Kobayashi, U. Andrae, M. A. Balmaseda, , G. Balsamo, P. Bauer, P. Bechtold, A. C. M. Beljaars, L. van de Berg, J. Bidlot, N. Bormann, C. Delsol, R. Dragani, M. Fuentes, A. J. Geer, L. Haimbergere, S. B. Healy, H. Hersbach, E. V. Holm, L. Isaksen, P. Kållberg, M. Köhler, M. Matricardi, A. P. McNally, B. M. Monge-Sanz, J.-J. Morcrette, B.-K. Park, C. Peubey, P. de Rosnay, C. Tavolato, J.-N. Thépaut, and F. Vitarta (2011), The ERA-Interim reanalysis: Configuration and performance of the data assimilation system, *Q. J. R. Meteorolog. Soc.*, *137*, 553–597, doi:10.1002/qj.828.

Dimri, A. P., D. Niyogi, A. P. Barros, J. Ridley, U. C. Mohanty, T. Yasunari, and D. R. Sikka (2015), Western Disturbances: A Review, *Rev. Geophys.*, *53*(2), 225–246, doi: 10.1002/2014RG000460.

Döll, P., F. Kaspar, and B. Lehner (2003), A global hydrological model for deriving water availability indicators: model tuning and validation, *J. Hydrol.*, *207*, 105–134, doi:10.1016/S0022-1694(02)00283-4.

Döll, P., H. Müller Schmied, C. Schuh, F. Portmann, and A. Eicker (2014), Global-scale assessment of groundwater depletion and related groundwater abstractions: Combining hydrological modeling with information from well observations and GRACE satellites, *Water Resour. Res.*, *50*(7), 5698–5720, doi:10.1002/2014WR015595.

FAO (2011), Ganges-brahmaputra-meghna basin, *Tech. Rep. Water Report 37*, AQUASTAT, Food and Agriculture Organization of the United Nations, Rome, Italy, available from: `http://www.fao.org/nr/water/aquastat/basins/gbm/index.stm`. Accessed on 21 Feb 2015.

Goswami, B. B., P. Mukhopadhyay, R. Mahanta, and B. N. Goswami (2010), Multiscale interaction with topography and extreme rainfall events in the northeast Indian region, *J. Geophys. Res.*, *115*(D12), doi:10.1029/2009JD012275.

Harris, I., P. Jones, T. Osborn, and D. Lister (2013), Updated high-resolution grids of monthly climatic observations- the CRU TS3.10 Dataset, *Int. J. Climatol.*, *34*(3), 623–642, doi:10.1002/joc.3711.

Hirschi, M., S. I. Seneviratne, V. Alexandrov, F. Boberg, C. Boroneant, O. B. Christensen, H. Formayer, B. Orlowsky, and P. Stepanek (2011), Observational evidence for soil-moisture impact on hot extremes in southeastern Europe, *Nature*, *4*, 1721, doi:10.1038/

723 ngeo1032.

724 Houborg, R., M. Rodell, B. Li, R. Reichle, and B. F. Zaitchik (2012), Drought
725 indicators based on model-assimilated Gravity Recovery and Climate Experiment
726 (GRACE) terrestrial water storage observations, *Water Resour. Res.*, *48*(7), doi:
727 10.1029/2011WR011291.

728 Huffman, G. J., D. T. Bolvin, E. J. Nelkin, D. B. Wolff, R. F. Adler, G. Gu, Y. Hong, K. P.
729 Bowman, and E. F. Stocker (2007), The TRMM Multisatellite Precipitation Analysis
730 (TMPA): Quasi-Global, Multiyear, Combined-Sensor Precipitation Estimates at Fine
731 Scales, *J. Hydrometeorol.*, *8*(1), 38–55, doi:10.1175/JHM560.1.

732 IPCC (2012), Managing the Risks of Extreme Events and Disasters to Advance Cli-
733 mate Change Adaptation, p. 582, Intergovernmental Panel on Climate Change, Geneva,
734 Switzerland.

735 Jacob, T., J. Wahr, W. T. Pfeffer, and S. Swenson (2012), Recent contributions of glaciers
736 and ice caps to sea level rise, *Nature*, *482*, 514–518, doi:10.1038/nature10847.

737 Jiménez-Cisneros, B. E., T. Oki, N. Arnell, G. Benito, J. Cogley, P. Döll, T. Jiang, and
738 S. Mwakalila (2014), Freshwater resources, in *Climate Change 2014: Impacts, Adapta-*
739 *tion, and Vulnerability. Part A: Global and Sectoral Aspects. Contribution of Working*
740 *Group II to the Fifth Assessment Report of the Intergovernmental Panel on Climate*
741 *Change*, edited by V. Barros, C. Field, D. Dokken, M. Mastrandrea, K. Mach, T. Bilir,
742 M. Chatterjee, K. Ebi, Y. Estrada, R. Genova, B. Girma, E. Kissel, A. Levy, S. Mac-
743 Cracken, P. Mastrandrea, and L. White, pp. 229–269, Cambridge University Press,
744 Cambridge, United Kingdom and New York, USA.

Kendall, M. G. (1962), Rank correlation methods, *J. Am. Stat. Assoc.*, *63*(324), 1379–1389, doi:10.1080/01621459.1968.10480934.

Khandu, E. F., J. L. Awange (2015), An evaluation of high-resolution gridded precipitation products over Bhutan (1998-2012), *Int. J. Climatol.*, doi:10.1002/joc.4402, available online at: `www.willy.com`.

Klein Tank, A. M. G., T. C. Peterson, D. A. Quadir, S. Dorji, X. Zou, H. Tang, K. Santhosh, U. R. Joshi, A. K. Jaswal, R. K. Kolli, A. B. Sikder, N. R. Deshpande, J. V. Revadekar, K. Yeleuova, S. Vandasheva, M. Faleyeva, P. Gomboluudev, K. P. Budhathoki, A. Hussain, M. Afzaal, L. Chandrapala, H. Anvar, D. Amanmurad, V. S. Asanova, P. D. Jones, M. G. New, , and T. Spektorman (2006), Changes in daily temperature and precipitation extremes in central and south Asia, *J. Geophys. Res.*, *111*(D16105), doi:10.1029/2005JD006316.

Kusche, J., R. Schmidt, S. Petrovic, and R. Rietbroek (2009), Decorrelated grace time-variable gravity solutions by GFZ, and their validation using a hydrological model, *J. Geod.*, *83*(10), 903–913, doi:10.1007/s00190-009-0308-3.

Landerer, F. W., and S. C. Swenson (2012), Accuracy of scaled GRACE terrestrial water storage estimates, *Water Resour. Res.*, *48*(W04531), doi:10.1029/2011WR011453.

Lau, W. K. M., K. M. Kim, C. N. Hsu, and B. N. Holben (2009), Possible influences of air pollution, dust- and sandstorms on the Indian monsoon, *Bull. - World Meteorological Organization*, *58*(1), 22–30.

Long, D., B. R. Scanlon, L. Longuevergne, A. Y. Sun, D. N. Fernando, and H. Save (2013), GRACE satellite monitoring of large depletion in water storage in response to the 2011 drought in Texas, *Geophys. Res. Lett.*, *40*(13), 3395–3401, doi:10.1002/grl.50655.

768 Long, D., Y. Shen, A. Sun, Y. Hong, L. Longuevergne, Y. Yang, B. Li, and L. Chen
769 (2014), Drought and flood monitoring for a large karst plateau in Southwest China
770 using extended GRACE data, *Remote Sens. Environ.*, *155*, 145–160, doi:10.1016/j.rse.
771 2014.08.006.

772 Mann, H. B. (1945), Nonparametric tests against trend, *Econometrica*, *13*(3), 245–259.

773 Matsuo, K., and K. Heki (2010), Time-variable ice loss in Asian high mountains from
774 satellite gravimetry, *Nat. Geosci.*, *290*, 30–36, doi:10.1016/j.epsl.2009.11.053.

775 McKee, T., N. J. Doesken, and J. Kliest (1993), The relationship of drought frequency and
776 duration to time scales, in *Proceedings of the 8th Conference of Applied Climatology,*
777 *17-22 January, Anaheim, CA*, pp. 194–184, American Meterological Society, Boston,
778 MA.

779 Mirza, M. M. Q., R. Warrick, N. Ericksen, and G. Kenny (1998), Trends and persistence
780 in precipitation in the Ganges, Brahmaputra and Meghna river basins, *Hydrol. Sci. J.*,
781 *43*(6), doi:10.1080/02626669809492182.

782 Mishra, V., R. Shah, and B. Thrasher (2014b), Soil moisture droughts under the ret-
783 rospective and projected climate in India, *J. Hydrometeorol.*, *15*, 2267–2292, doi:
784 10.1175/JHM-D-13-0177.1.

785 Miyan, M. A. (2014), Droughts in Asian least developed countries: Vulnerability and
786 sustainability, *Wea. and Clim. Ext.*, *7*, 8–23, doi:10.1016/j.wace.2014.06.003, in Press.

787 Müller Schmied, H., S. Eisner, D. Franz, M. Wattenbach, F. Portmann, M. Flörke, and
788 P. Döll (2014), Sensitivity of simulated global-scale freshwater fluxes and storages to
789 input data, hydrological model structure, human water use and calibration, *Hydrol.*
790 *Earth. Syst. Sci.*, *18*, 3511–3538, doi:10.5194/hess-18-3511-2014.

Papa, F., F. Frappart, Y. Malbeteau, M. Shamsudduha, V. Vuruputur, M. Sekhar, G. Ramillien, C. Prigent, F. Aires, R. K. Pandey, S. Bala, and S. Calmant (2015), Satellite-derived surface and sub-surface water storage in the Ganges-Brahmaputra River Basin, *J. Hydrol.*, doi:10.1016/j.ejrh.2015.03.004, in Press.

Pervez, M. S., and G. M. Henebry (2015), Spatial and seasonal responses of precipitation in the Ganges and Brahmaputra river basins to ENSO and Indian Ocean dipole modes: Implications for flooding and drought, *Natural Hazards and Earth System Science*, *15*, 147–162, doi:10.5194/nhess-15-147-2015.

Rajeevan, M., and J. Bhate (2008), A high resolution daily gridded rainfall data set (1971-2005) for mesoscale meteorological studies, *Tech. Rep. NCC Research Report No. 9*, National Climate Centre, Indian Meteorological Department, Pune, India, available from `http://www.imdpune.gov.in/ncc_rept/RESEARCH\%20REPORT\%209.pdf`, accessed on: 21 June 2014.

Ramanathan, V., C. Chung, D. Kim, T. Bettge, L. Buja, J. T. Kiehl, W. M. Washington, Q. Fu, D. R. Sikka, , and M. Wild (2005), Atmospheric brown clouds: Impacts on South Asian climate and hydrological cycle, *PNAS*, *102*(15), 5326–5333, doi: 10.1073pnas.0500656102.

Richey, A., B. Thomas, M. Lo, J. T. Reager, J. S. Famiglietti, K. Voss, S. Swenson, and M. Rodell (2015), Quantifying renewable groundwater stress with GRACE, *Water Resour. Res.*, *51*, 1–20, doi:10.1002/2015WR017349.

Rienecker, M. M., M. J. Suarez, R. Gelaro, R. Todling, J. Bacmeister, E. Liu, M. G. Bosilovich, S. D. Schubert, L. Takacs, G. K. Kim, S. Bloom, J. Chen, D. Collins, A. Conaty, A. da Silva, W. Gu, J. Joiner, R. D. Koster, R. Lucchesi, A. Molod,

T. Owens, S. Pawson, P. Pegion, C. R. Redder, R. Reichle, F. R. Robertson, A. G. Ruddick, M. Sienkiewicz, and J. Woollen (2011), MERRA: NASA's Modern-Era Retrospective Analysis for Research and Applications, *J. Clim.*, *24*(14), 3624–3648, doi: 10.1175/JCLI-D-11-00015.1.

Rodell, M., P. R. H. U. Jambor, J. Gottschalck, K. Mitchell, C.-J. Meng, K. Arsenault, B. Cosgrove, J. Radakovich, M. Bosilovich, J. K. Entin, J. P. Walker, D. Lohmann, and D. Toll (2004), The Global Land Data Assimilation System, *Bull. Am. Meteorol. Soc.*, *85*, 381–394, doi:10.1175/BAMS-85-3-381.

Rodell, M., I. Velicogna, and J. S. Famiglietti (2009), Satellite-based estimates of groundwater depletion in India, *Hydrol. Earth Syst. Sci.*, *460*, 999–1002, doi:10.1038/ nature08238.

Roy, S. S., and R. C. Balling (2004), Trends in extreme daily precipitation indices in India, *Int. J. Climatol.*, *24*(4), 457–466, doi:10.1002/joc.995.

Saji, N. H., B. N. Goswami, P. N. Vinayachandran, and T. Yamagata (1999), A dipole mode in the tropical Indian Ocean, *Nature*, *401*, 360–363.

Scherler, D., B. Bookhagen, and M. R. Strecker (2011), Spatially variable response of Himalayan glaciers to climate change affected by debris cover, *Nat. Geosci.*, *4*, 156–159, doi:10.1038/ngeo1068.

Schneider, U., A. Becker, P. Finger, A. M.-. Christoffer, M. Ziese, and B. Rudolf (2014), GPCC's new land surface precipitation climatology based on quality-controlled in situ data and its role in quantifying the global water cycle, *Theor. Appl. Climatol.*, *115*(1-2), 15–40, doi:10.1007/s00704-013-0860-x.

836 Shahid, S. (2011), Trends in extreme rainfall events of Bangladesh, *Theor. Appl. Climatol.*,
837 *104*(3-4), 489–499, doi:10.1007/s00704-010-0363-y.
838 Shamsudduha, M. (2013), Groundwater resilience to human development and climate
839 change in south asia, *Groundwater Forum*.
840 Shamsudduha, M., R. E. Chandler, R. G. Taylor, and K. M. Ahmed (2009a), Re-
841 cent trends in groundwater levels in a highly seasonal hydrological system: the
842 Ganges-Brahmaputra-Meghna Delta, *Hydrol. Earth Syst. Sci.*, *13*, 2373–2385, doi:
843 10.5194/hess-13-2373-2009.
844 Shamsudduha, M., R. G. Taylor, and R. E. Chandler (2009b), Monitoring groundwater
845 storage changes in the highly seasonal humid tropics: Validation of GRACE measure-
846 ments in the Bengal Basin, *Water Resour. Res.*, *48*(2), doi:10.1029/2011WR010993.
847 Shum, C. K., J. Y. Guo, F. Hossain, J. Duan, D. E. Alsdorf, C. Y. K. X. J. Duan, H. Lee,
848 M. Schmidt, and L. Wang (2011), Inter-annual water storage changes in Asia from
849 GRACE data, in *Climate Change and Food Security in South Asia*, edited by R. Lal,
850 M. V. K. Sivakumar, S. M. A. Faiz, A. H. M. M. Rahman, and K. R. Islam, chap. 6,
851 pp. 69–83, Springer Netherlands.
852 Steckler, M. S., S. L. Nooner, S. H. Akhter, S. K. Chowdhury, S. Bettadpur, L. Seeber,
853 and M. G. Kogan (2010), Modeling Earth deformation from monsoonal flooding in
854 Bangladesh using hydrographic, GPS, and Gravity Recovery and Climate Experiment
855 (GRACE) data, *J. Geophys. Res.*, *15*(B8), doi:10.1029/2009JB007018.
856 Tapley, B. D., S. Bettadpur, M. Watkins, and C. Reigber (2004), The gravity recovery
857 and climate experiment: Mission overview and early results, *Geophys. Res. Lett.*, *33*,
858 doi:10.1029/2004GL019779.

Taylor, R. G., M. C. Todd, L. Kongola, L. Maurice, E. Nahozya, H. Sanga, and A. M. MacDonald (2013), Evidence of the dependence of groundwater resources on extreme rainfall in East Africa, *Nat. Clim. Chang.*, *3*, 374378, doi:10.1038/nclimate1731.

Thomas, A. C., J. T. Reager, J. S. Famiglietti, and M. Rodell (2014), A GRACE-based water storage deficit approach for hydrological drought characterization, *Geophys. Res. Lett.*, *41*(5), 1537–1545, doi:10.1002/2014GL059323.

Tiwari, V. M., J. Wahr, and S. Swenson (2009), Dwindling groundwater resources in northern India, from satellite gravity observations, *Geophys. Res. Lett.*, *36*(L18401), doi:10.1029/2009GL039401.

Turner, A. G., and H. Annamalai (2012), Climate change and the South Asian summer monsoon, *Nat. Clim. Chang.*, *2*, 587–595, doi:10.1028/nclimate1495.

van den Dool, H., J. Huang, and Y. Fan (2003), Performance and analysis of the constructed analogue method applied to US soil moisture applied over 1981-2001, *Geophys. Res. Lett.*, *108*(8617), doi:10.1029/2002JD003114.

Wahr, J., M. Molenaar, and F. Bryan (1998), Time variability of the Earth's gravity field: Hydrological and oceanic effects and their possible detection using GRACE, *J. Geophys. Res.*, *103*(B12), 30,205–30,229, doi:10.1029/98JB02844.

Wouters, B., J. A. Bonin, D. P. Chambers, R. E. M. Riva, I. Sasgen, and J. Wahr (2014), GRACE, time-varying gravity, Earth system dynamics and climate change, *Reports on Progress in Physics*, *77*(11), 116,801, doi:10.1088/0034-4885/77/11/116801.

Yatagai, A., K. Kamiguchi, O. Arakawa, A. Hamada, N. Yasutomi, and A. Kitoh (2012), APHRODITE: Constructing a Long-term Daily Gridded Precipitation Dataset for Asia based on a Dense Network of Rain Gauges, *Bull. Am. Meteorol. Soc.*, doi:10.1175/

882 BAMS-D-11-00122.1.

Figure 1. Overview of the GBM River Basin in South Asia. The digital elevation model was derived from the Shuttle Radar Topography Mission (SRTM, `http://srtm.csi.cgiar.org`).

Figure 2. Spatial variability of long-term trends in monthly rainfall based on various products over the GBM River Basin. The long-term trends were derived from (a) APHRODITE (1979-2007), (b) GPCCv6 (1979-2007), (c) CRU_TS3.22 (1979-2007), and for the TRMM-era (1998-2014), trends were computed for (d) CRU_TS3.22 (1998-2013) and (e) TMPAv7 (1998-2014). Note that only those values significant at 95% confidence level are shown. The blue and black polygons represent the boundaries of Ganges and Brahmaputra-Meghna basin, used hereafter in all the spatial maps.

Figure 3. Linear trends in monthly soil moisture data derived from three global re-analyses:(a) MERRA, (b) ERA-Interim, and (c) CPC for the period 1980-2014.

Figure 4. Changes in TWS for the period 2002-2014. The results were based on the average of GRACE Level 2 products from CSR, GFZ, and JPL. Note that only those values significant at 95% confidence level are shown.

Figure 5. Linear trend in surface water storage simulated by WGHM for the periods (a) 1979-2009, and (b) 2002-2009.

Figure 6. Trends and variabilities of TWS over (a) Ganges and (b) Brahmaputra River Basin from 2002-2014. The seasonal cycles were removed in order to indicate the linear trends.

Figure 7. Signal-to-noise ratio of various soil moisture products derived by dividing the RMS grid values by the respective error magnitudes estimated by the TCH method: (a) MERRA, (b) ERA-Interim, and (c) CPC.

Figure 8. Temporal correlations and lag times between GRACE-derived TWS changes, soil moisture, and rainfall in the GBM River Basin. The correlations were computed for the GRACE data period of 2002-2014.

Figure 9. Interannual variability of basin-averaged monthly rainfall, soil moisture, and GRACE-derived TWS changes in (a) Ganges, and (b) Brahmaputra River Basins. The basin-average time series were obtained by removing the linear trends and dominant annual and semi-annual amplitudes and a moving average of 6 months was applied .

Figure 10. Cumulative sums of basin-averaged monthly rainfall, soil moisture, and GRACE-derived TWS changes in (a) Ganges, and (b) Brahmaputra River Basins.

Figure 11. Standardised precipitation index (SPI) of rainfall and standardized indices (SIs) of soil moisture and TWS for the (a) Ganges and (b) Brahmaputra River Basins. These indices were derived based on 6-month running mean in order to show the medium to long-term extremes for the period 1980 to 2014 (2002-2014 for TWS).

Figure 12. Basin-averaged mean seasonal rainfall over Ganges and Brahmaputra-Meghna River Basins between 1980-2014. (a) June-September mean rainfall and (b) December-February mean rainfall.

Figure 13. RMS of difference between natural TWS and TWS under the influence of human water abstraction. .

Figure 14. Time series of natural TWS ("NOUSE", black dashed line), TWS under the influence of human water use ("IRR70_S", gray line) as simulated by WaterGAP, and their difference (black line). Linear trends are shown for 1979-2009, 1979-2001 and 2002-2009.

Table 1. Various categories of extreme rainfall events and drought based on SPI and SIs of soil moisture and TWS [see e.g., *McKee et al.*, 1993].

SPI/SI	**Category**
+2.0 and above	Extreme wet
+1.0 to +1.99	Very wet
+0.99 to -0.99	Normal
-1.0 to -1.99	Moderate drought
-2.0 and below	Extreme drought

Table 2. Uncertainties in precipitation (1998-2007), soil moisture (1979-2014), and GRACE TWS changes (2002-2014) in the two sub-basins of GBM River Basin estimated using the generalized TCH method. All the units are in mm/month.

River Basin	**Precipitation [1998-2007]**			
	APHRODITE	CRU_TS3.22	GPCCv6	TMPAv7
Ganges	16.3	20.0	8.8	14.1
Brahmaputra-Meghna	29.3	18.2	8.7	11.1
	Soil Moisture [1980-2014]			
	MERRA	ERA	CPC	
Ganges	10.6	26.1	35.7	
Brahmaputra-Meghna	8.8	62.3	14.77	
	GRACE TWS [2002-2014]			
	CSR	GFZ	JPL	
Ganges	4.3	14.8	12.8	
Brahmaputra-Meghna	6.4	13.1	14.4	

Table 3. Correlation coefficients and time lags between SPI (6-month) and SI of soil moisture and TWS in the GBM River Basin for the period 2002-2014.

Basin	**Ganges**		**Brahmaputra-Meghna**	
	Correlation	Lags (in months)	Correlation	Lags (in months)
Rainfall vs TWS	0.6	3	0.4	4
Soil moisture vs TWS	0.7	2	0.8	2
Rainfall vs soil moisture	0.8	2	0.6	3

Table 4. Duration and magnitudes of the drought events from 2002-2014.

SL	Variable	Period	Duration	Maximum Intensity	Drought Category
			Ganges		
	Precipitation	May 2005-Feb 2007	22 months	-1.8	Moderate
1	Soil moisture	Jun 2005- May 2007	24 months	-2.3	Extreme
	TWS	Feb 2006Jul 2008	24 months	-0.9	Normal
	Precipitation	Dec 2008-May 2011	29 months	-2.5	Extreme
2	Soil moisture	Jan 2009-Mar 2010	15 months	-2.0	Extreme
	TWS	Mar 2009-Aug 2011	29 months	-2.2	Extreme
			Brahmaputra-Meghna		
	Precipitation	Jan 2005-May 2007	29 months	-2.3	Moderate
1	Soil moisture	Jan 2005-Aug 2007	32 months	-1.9	Moderate
	TWS	Sept 2005June 2007	30 months	-2.5	Extreme
	Precipitation	Jan 2009-Mar 2010	16 months	-2.5	Extreme
2	Soil moisture	May 2009-May 2010	13 months	-0.6	Normal
	TWS	Jun 2009-Aug 2010	15 months	-1.9	Moderate

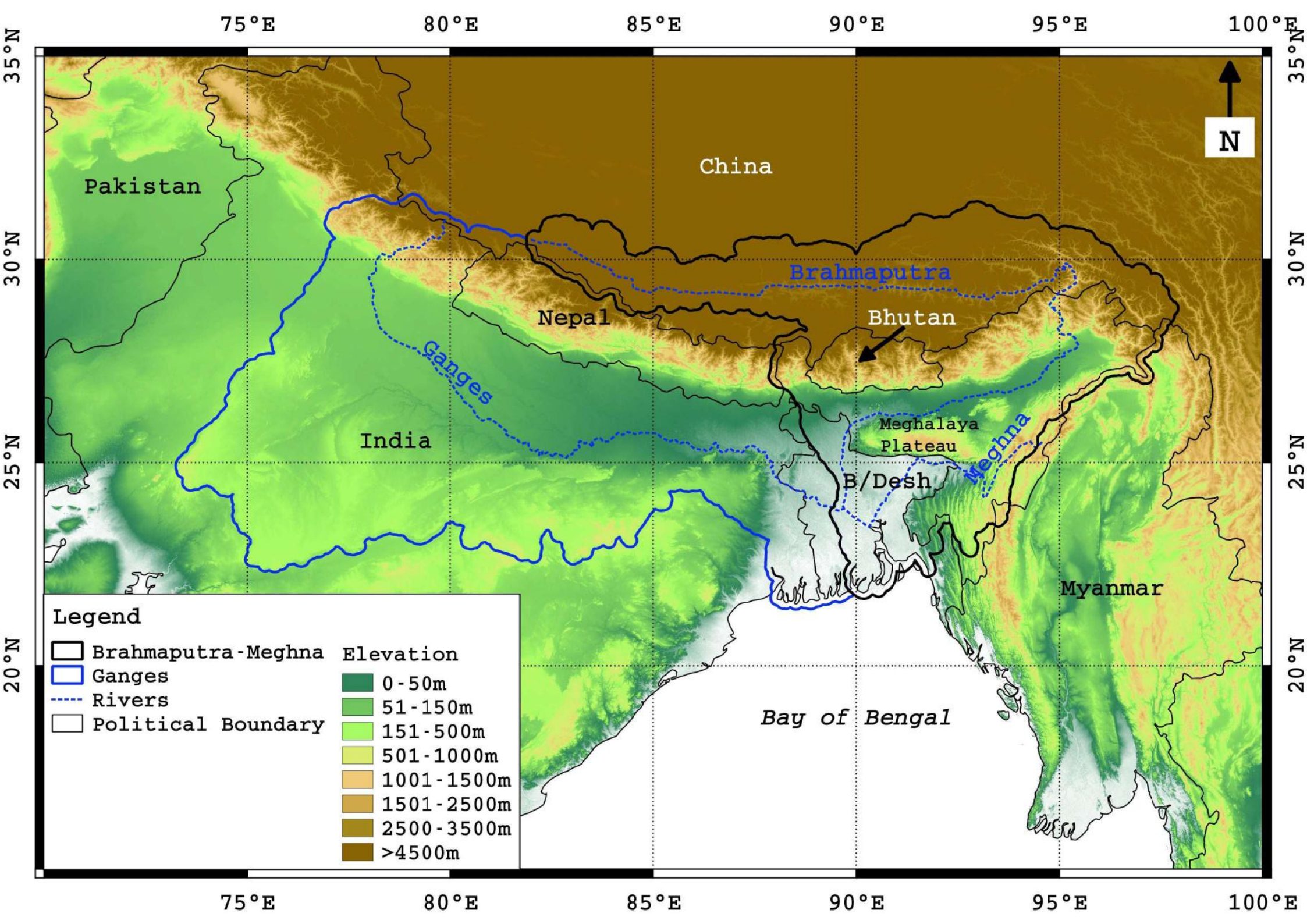
75°E
80°E
85°E
90°E
95°E
100°E
35°N
30°N
25°N
20°N
N
China
Pakistan
Brahmaputra
Nepal
Bhutan
Ganges
India
Meghalaya
Plateau
Meghna
B/Desh
Myanmar
Bay of Bengal
Legend
Brahmaputra-Meghna
Ganges
Rivers
Political Boundary
Elevation
0-50m
51-150m
151-500m
501-1000m
1001-1500m
1501-2500m
2500-3500m
>4500m

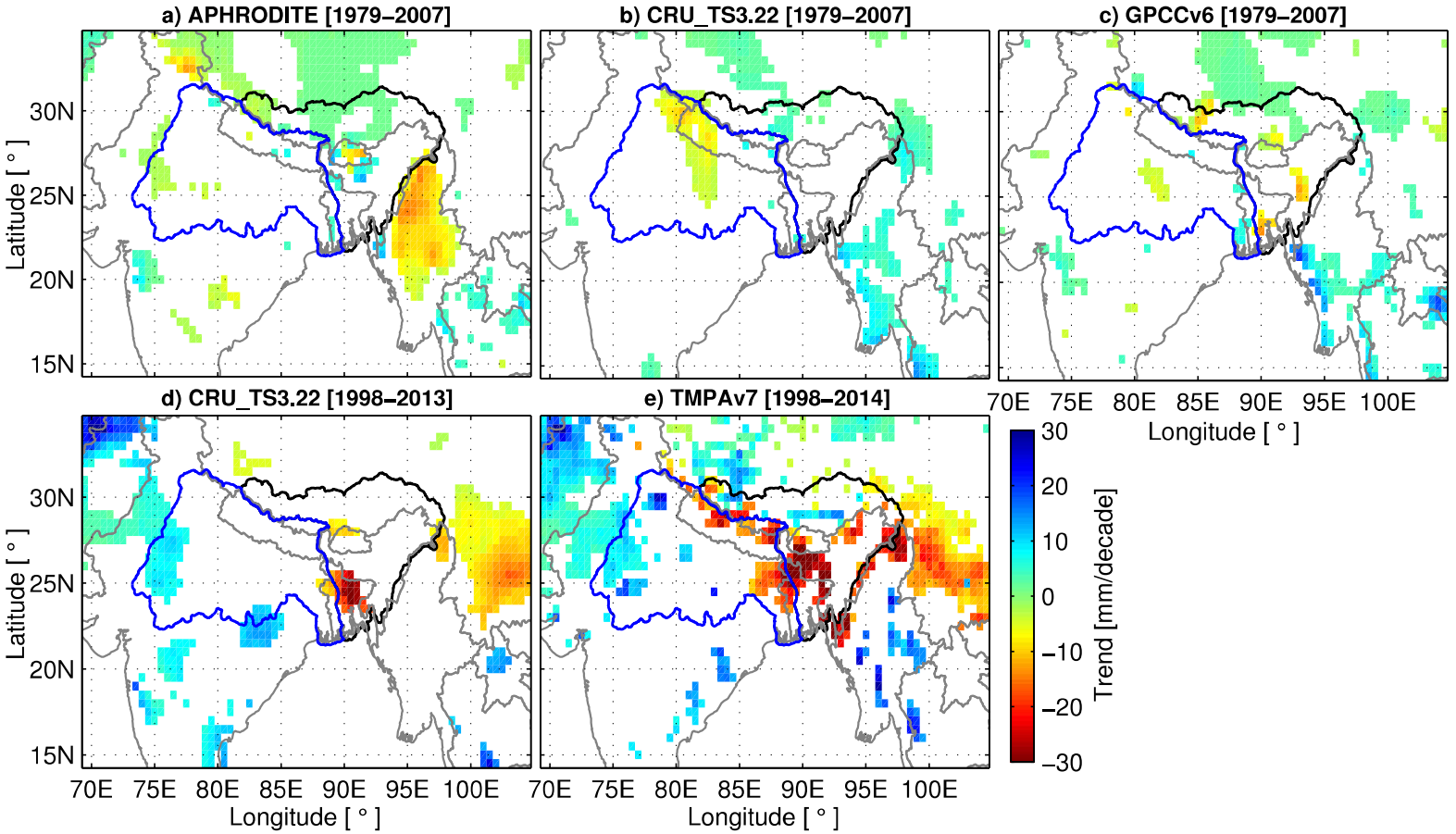
a) APHRODITE [1979–2007]
b) CRU_TS3.22 [1979–2007]
c) GPCCv6 [1979–2007]
d) CRU_TS3.22 [1998–2013]
e) TMPAv7 [1998–2014]
Latitude [°]
30N
25N
20N
15N
70E 75E 80E 85E 90E 95E 100E
Longitude [°]
Trend [mm/decade]
30
20
10
0
−10
−20
−30

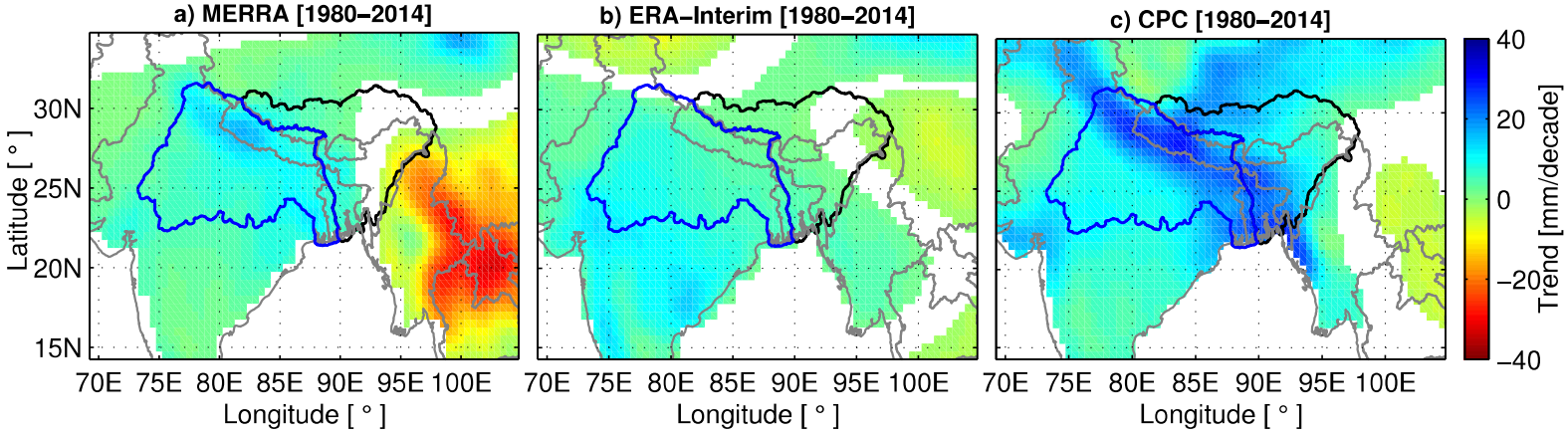
a) MERRA [1980–2014]
b) ERA–Interim [1980–2014]
c) CPC [1980–2014]
Latitude [°]
30N
25N
20N
15N
70E 75E 80E 85E 90E 95E 100E
Longitude [°]
Trend [mm/decade]
40
20
0
–20
–40

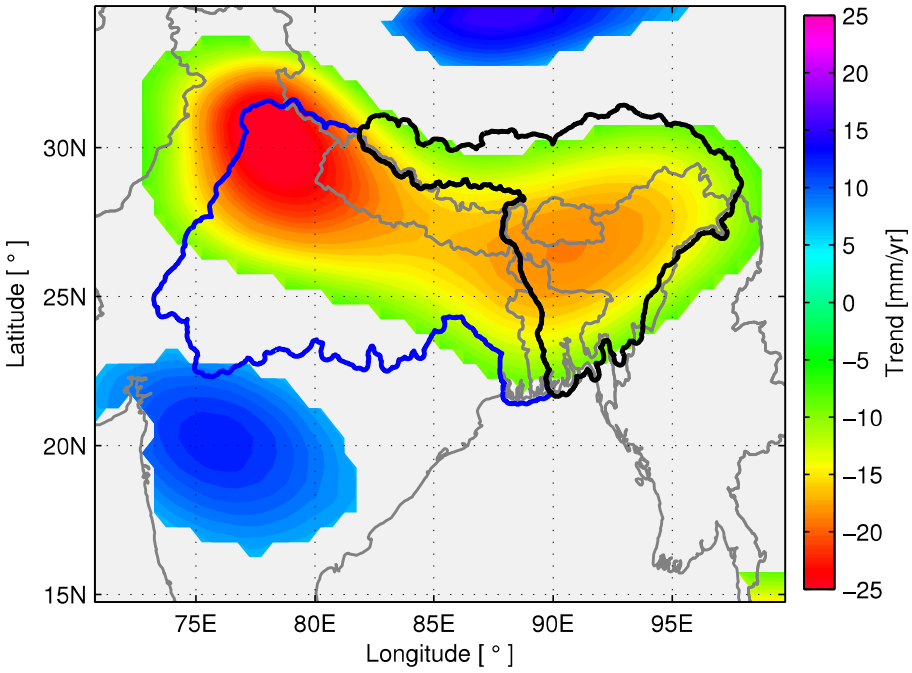
30N
25N
20N
15N
75E
80E
85E
90E
95E
Latitude [°]
Longitude [°]
25
20
15
10
5
0
−5
−10
−15
−20
−25
Trend [mm/yr]

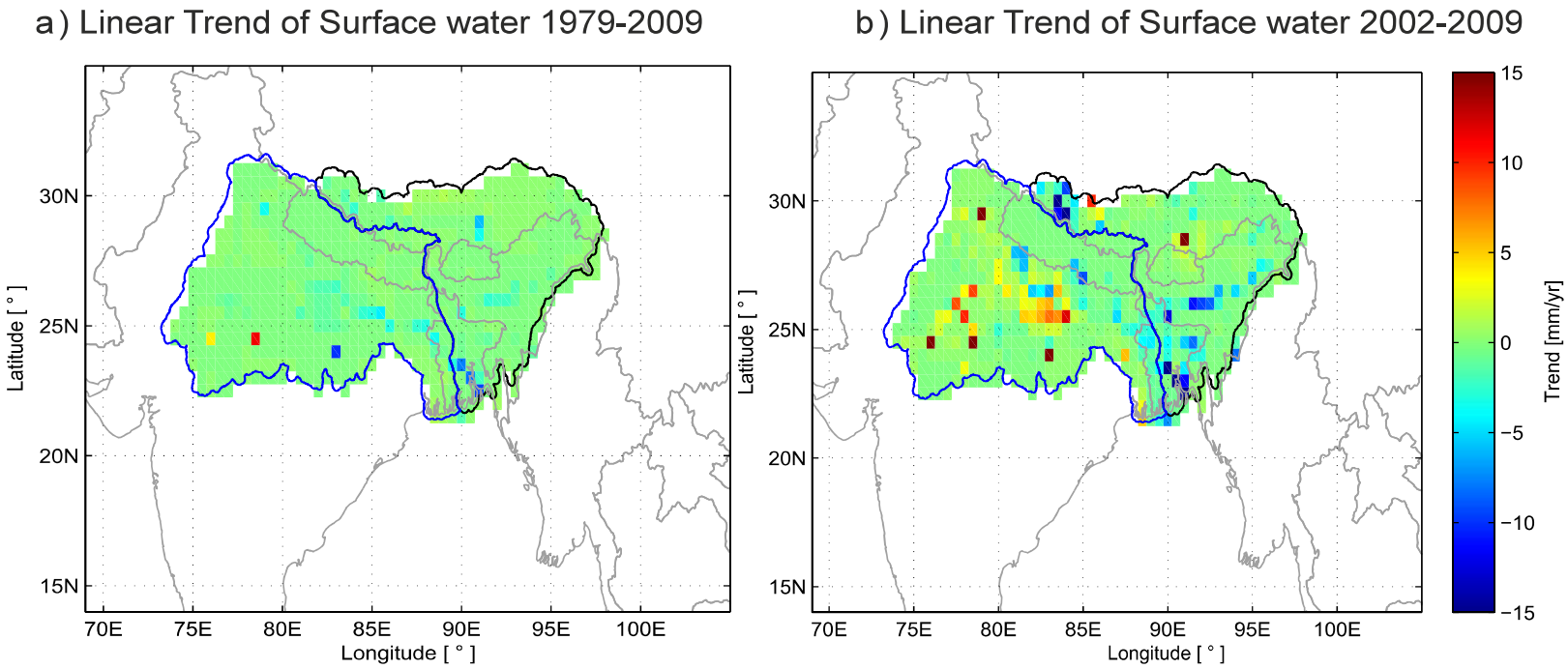
a) Linear Trend of Surface water 1979-2009
b) Linear Trend of Surface water 2002-2009
30N
25N
20N
15N
Latitude [°]
70E
75E
80E
85E
90E
95E
100E
Longitude [°]
15
10
5
0
−5
−10
−15
Trend [mm/yr]

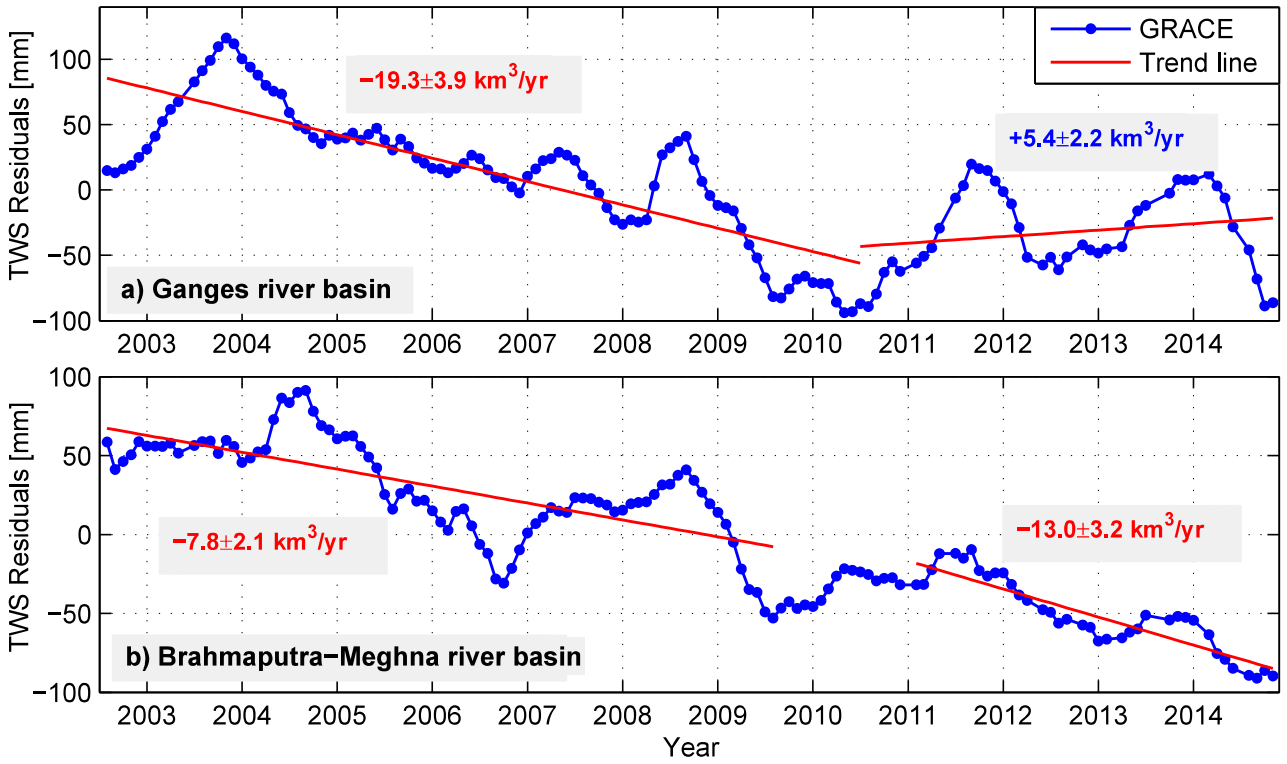
GRACE
Trend line
−19.3±3.9 km3/yr
+5.4±2.2 km3/yr
a) Ganges river basin
−7.8±2.1 km3/yr
−13.0±3.2 km3/yr
b) Brahmaputra−Meghna river basin
TWS Residuals [mm]
TWS Residuals [mm]
Year
100
50
0
−50
−100
2003
2004
2005
2006
2007
2008
2009
2010
2011
2012
2013
2014

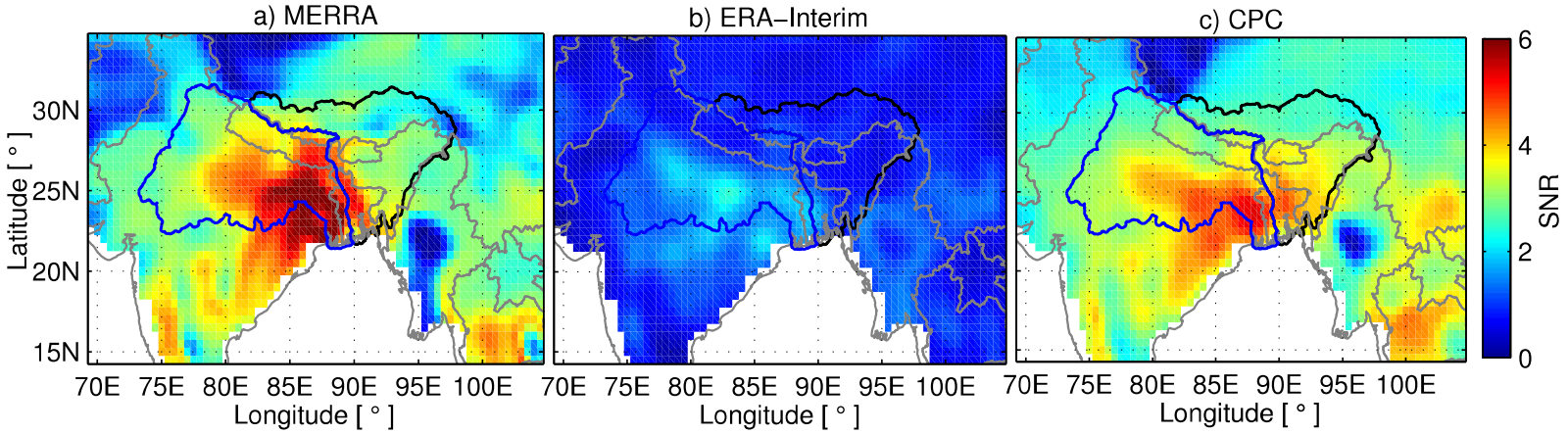
a) MERRA
b) ERA–Interim
c) CPC
Latitude [°]
30N
25N
20N
15N
70E 75E 80E 85E 90E 95E 100E
Longitude [°]
SNR
6
4
2
0

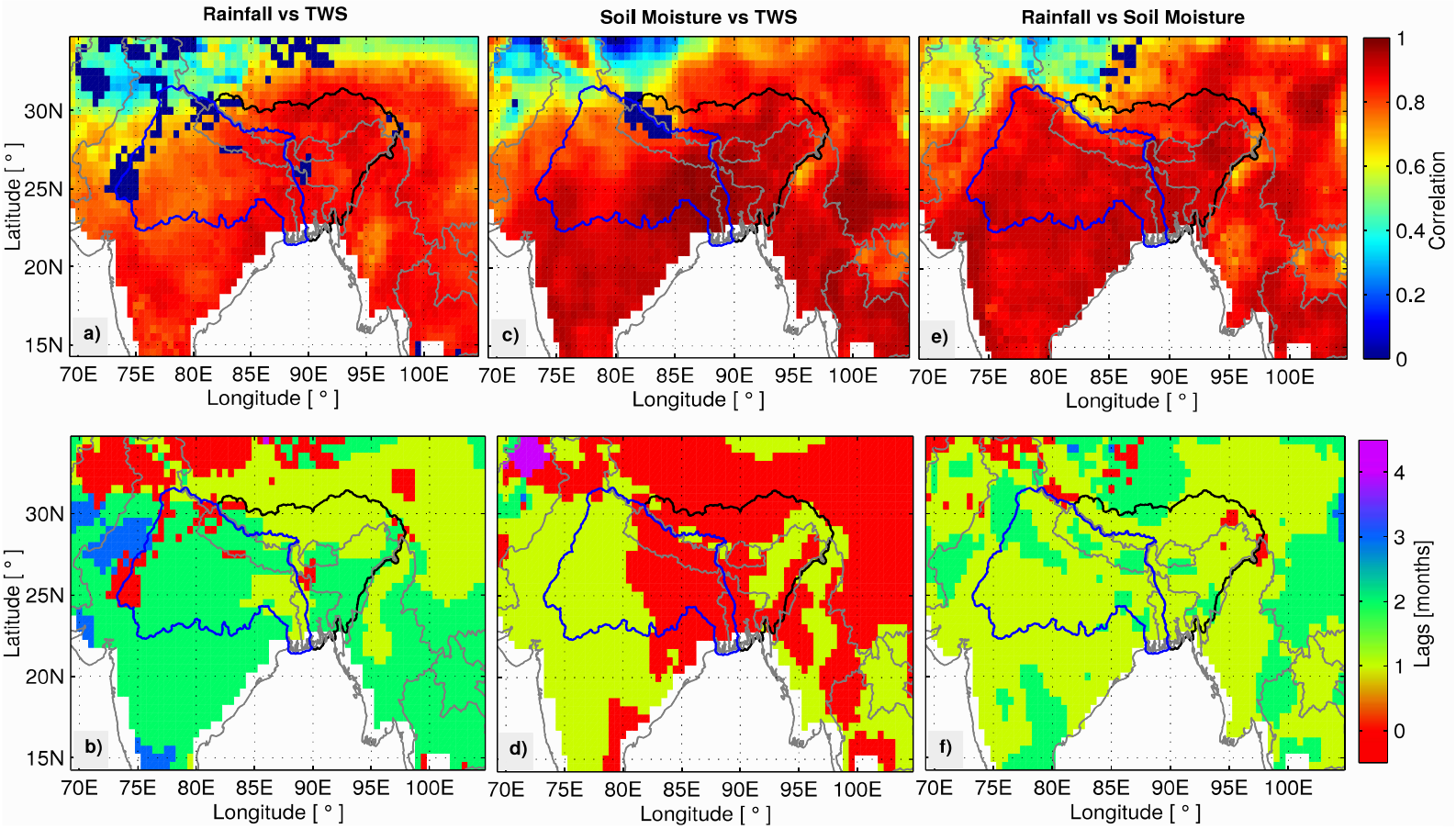
Rainfall vs TWS
Soil Moisture vs TWS
Rainfall vs Soil Moisture
a)
b)
c)
d)
e)
f)
30N
25N
20N
15N
Latitude [°]
70E 75E 80E 85E 90E 95E 100E
Longitude [°]
Correlation
1
0.8
0.6
0.4
0.2
0
Lags [months]
4
3
2
1
0

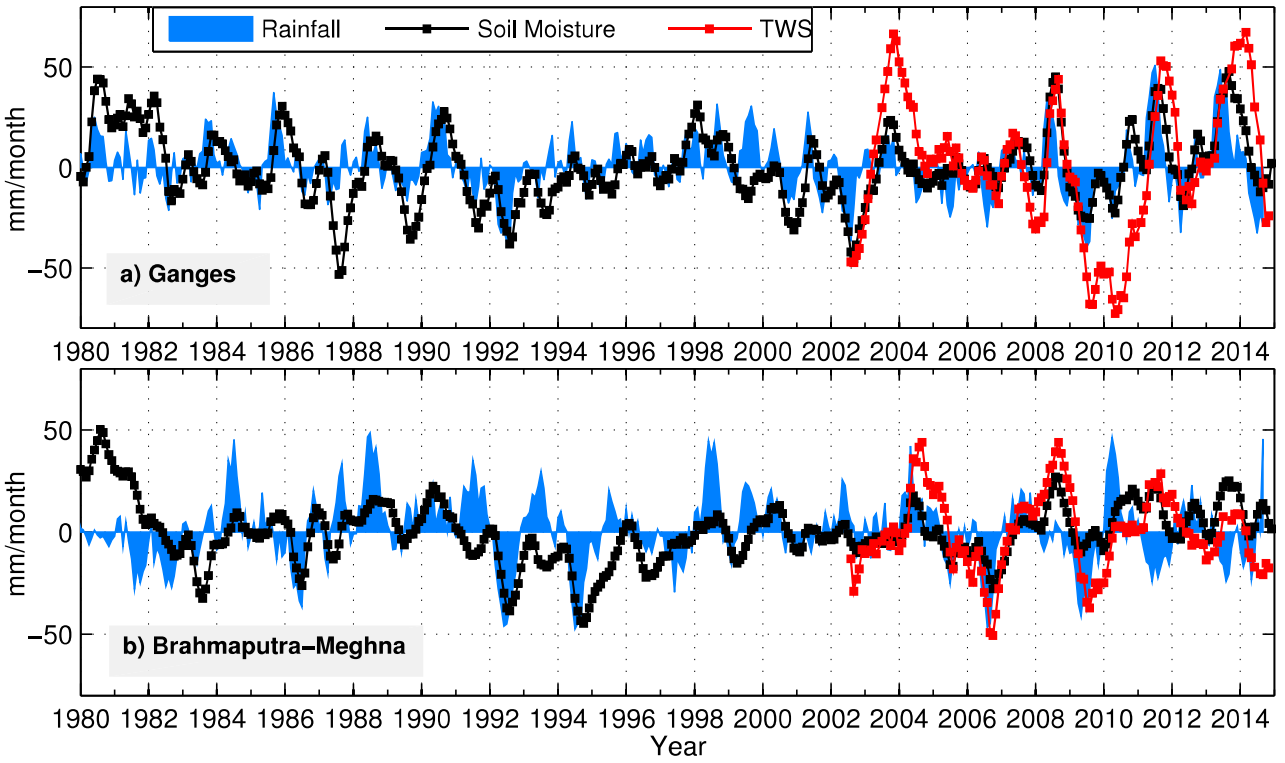
Rainfall
Soil Moisture
TWS
50
0
−50
mm/month
a) Ganges
1980 1982 1984 1986 1988 1990 1992 1994 1996 1998 2000 2002 2004 2006 2008 2010 2012 2014
50
0
−50
mm/month
b) Brahmaputra−Meghna
1980 1982 1984 1986 1988 1990 1992 1994 1996 1998 2000 2002 2004 2006 2008 2010 2012 2014
Year

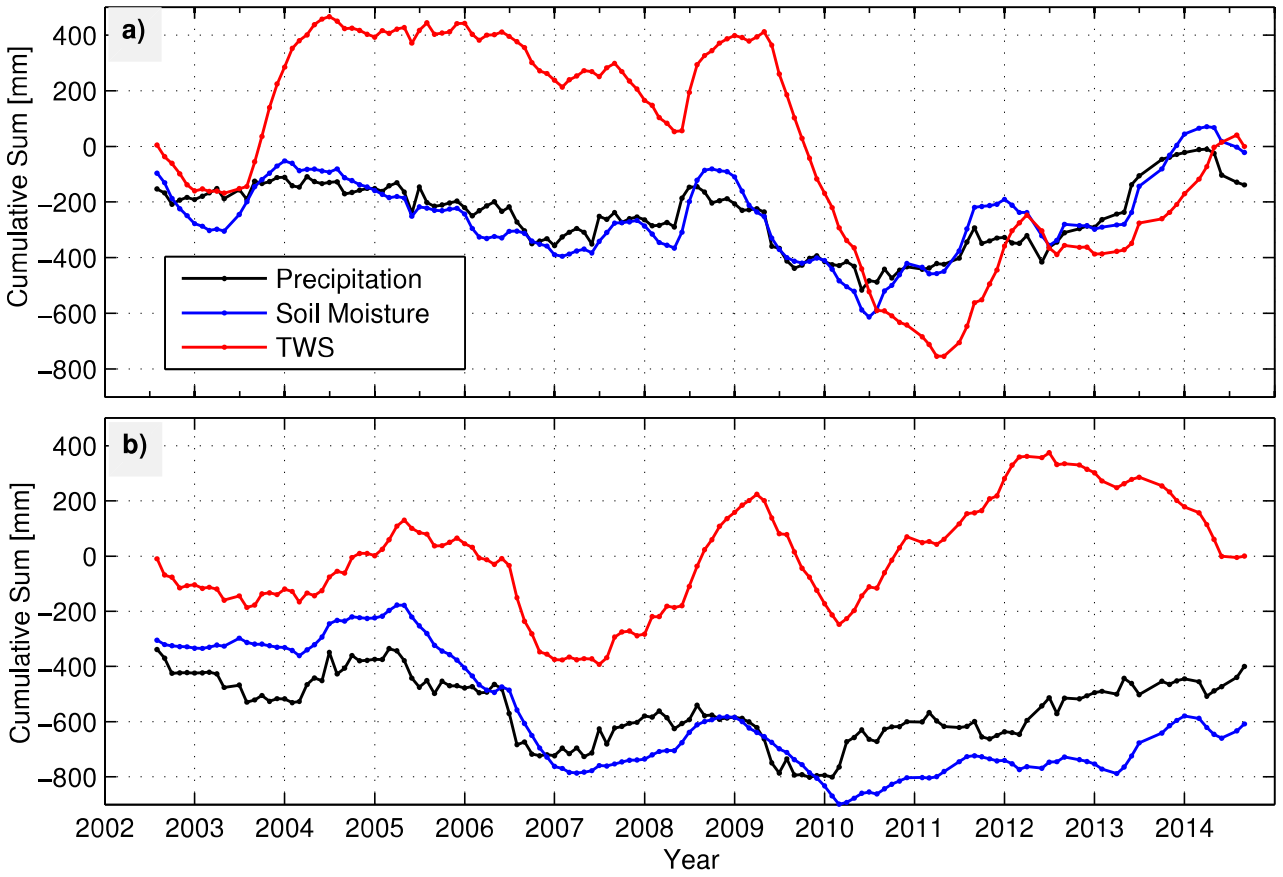
a)
b)
Cumulative Sum [mm]
400
200
0
−200
−400
−600
−800
Precipitation
Soil Moisture
TWS
2002
2003
2004
2005
2006
2007
2008
2009
2010
2011
2012
2013
2014
Year

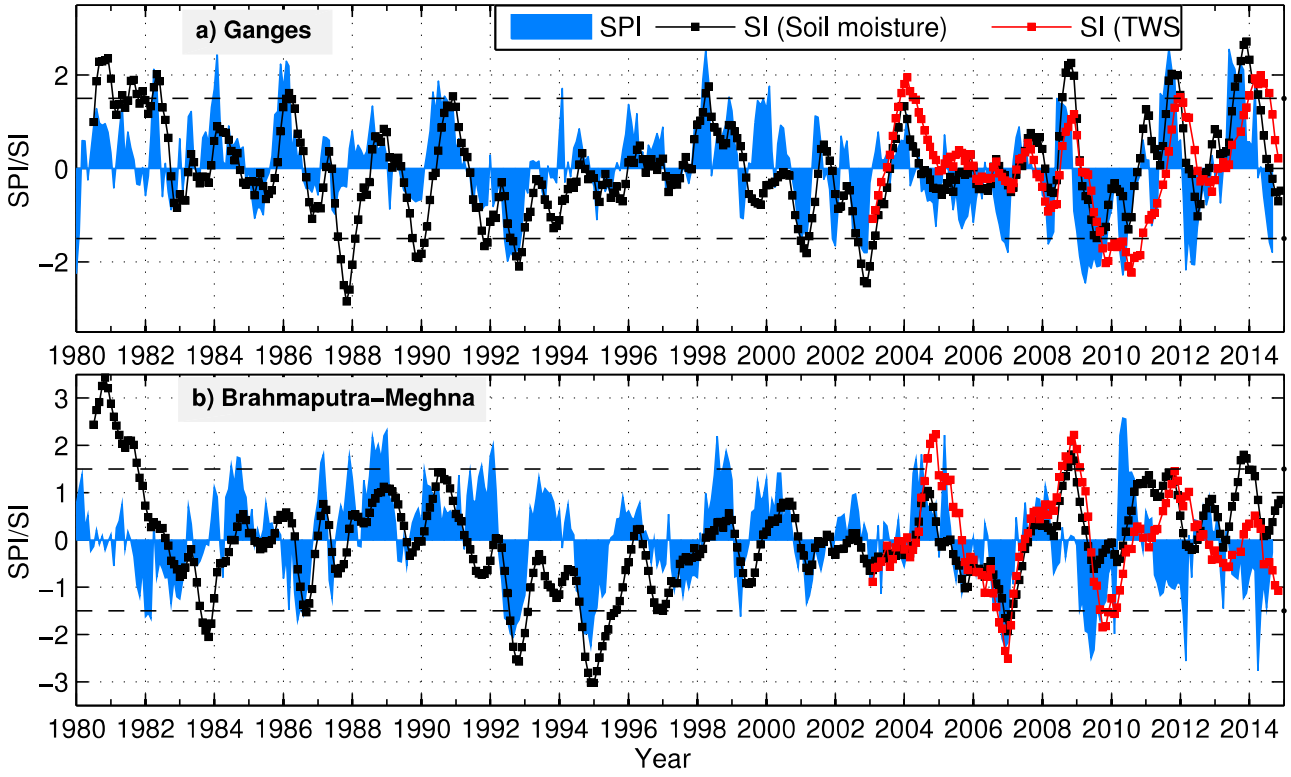
a) Ganges
SPI
SI (Soil moisture)
SI (TWS
SPI/SI
2
0
−2
1980 1982 1984 1986 1988 1990 1992 1994 1996 1998 2000 2002 2004 2006 2008 2010 2012 2014
b) Brahmaputra–Meghna
SPI/SI
3
2
1
0
−1
−2
−3
1980 1982 1984 1986 1988 1990 1992 1994 1996 1998 2000 2002 2004 2006 2008 2010 2012 2014
Year

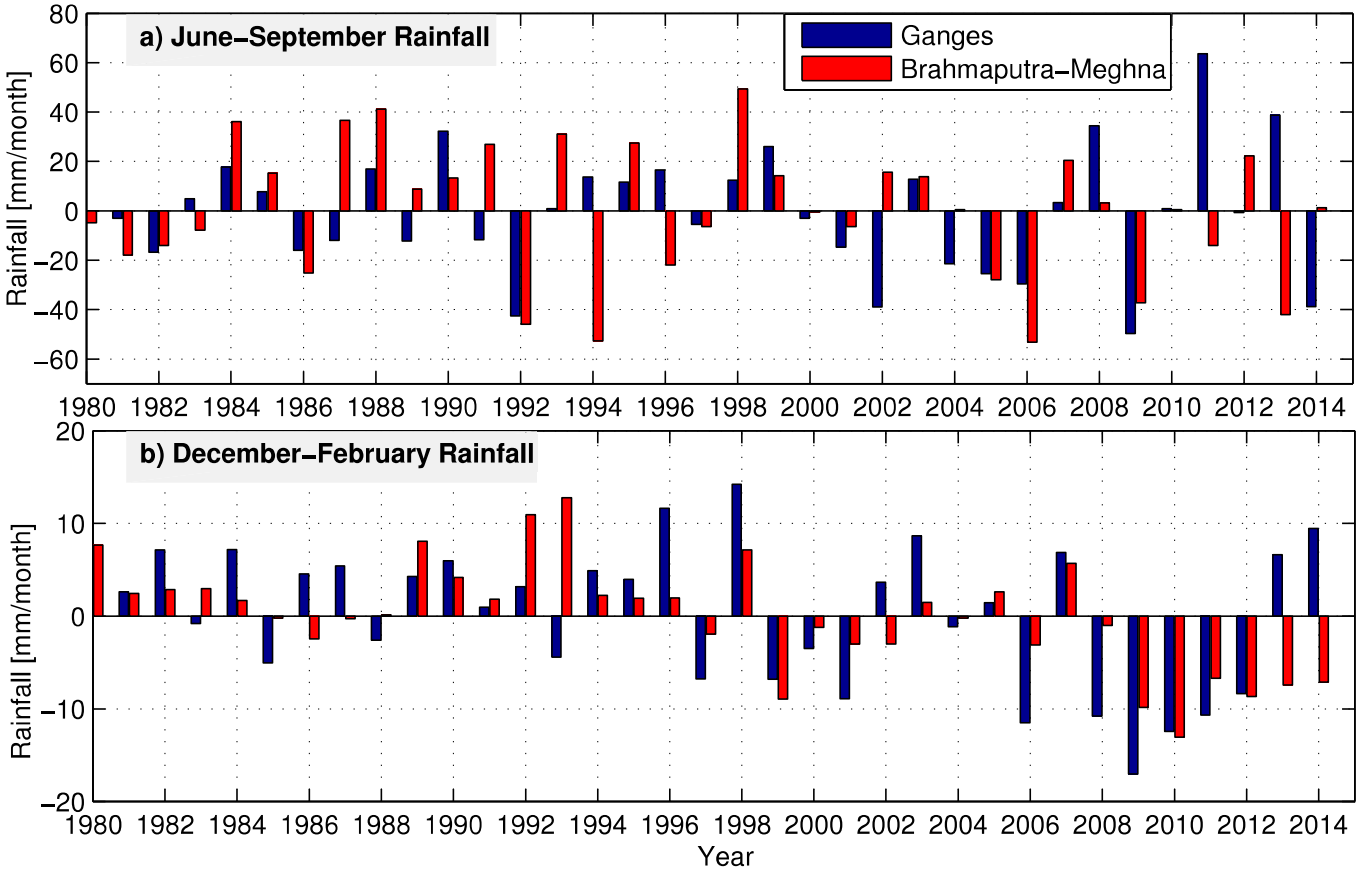
a) June–September Rainfall
Ganges
Brahmaputra–Meghna
Rainfall [mm/month]
80
60
40
20
0
−20
−40
−60
1980 1982 1984 1986 1988 1990 1992 1994 1996 1998 2000 2002 2004 2006 2008 2010 2012 2014
b) December–February Rainfall
Rainfall [mm/month]
20
10
0
−10
−20
1980 1982 1984 1986 1988 1990 1992 1994 1996 1998 2000 2002 2004 2006 2008 2010 2012 2014
Year

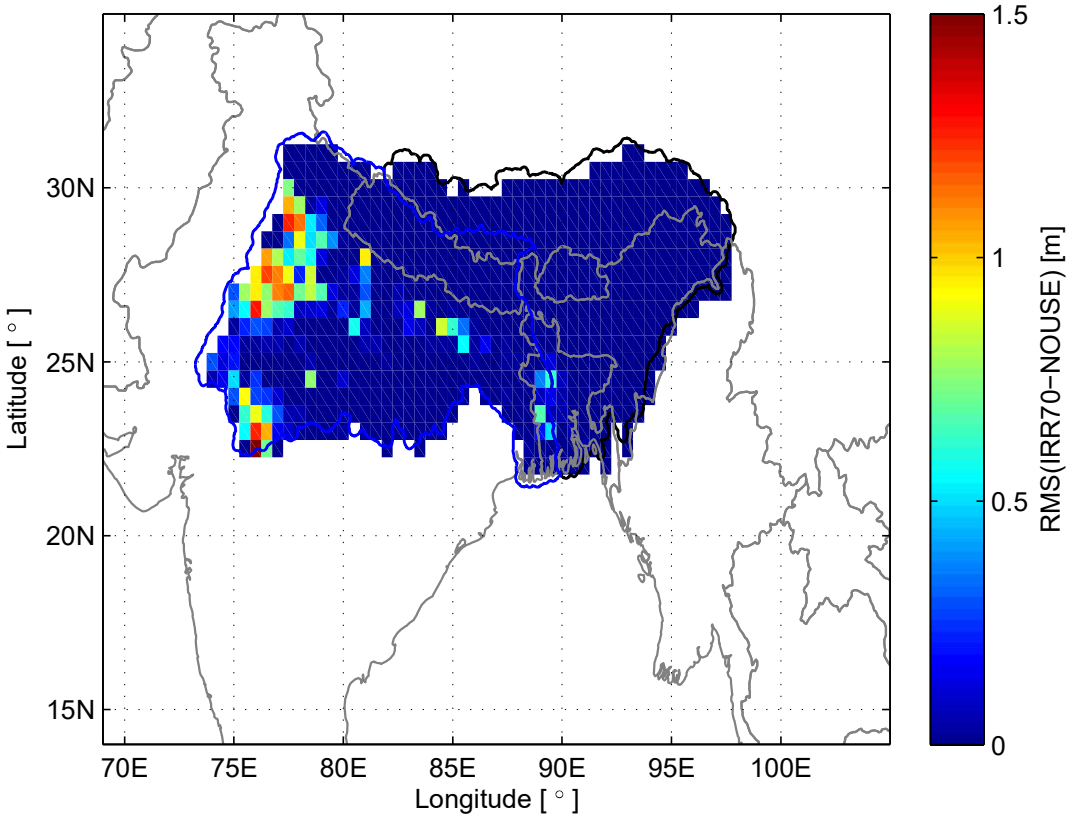
30N
25N
20N
15N
Latitude [°]
70E
75E
80E
85E
90E
95E
100E
Longitude [°]
1.5
1
0.5
0
RMS(IRR70−NOUSE) [m]

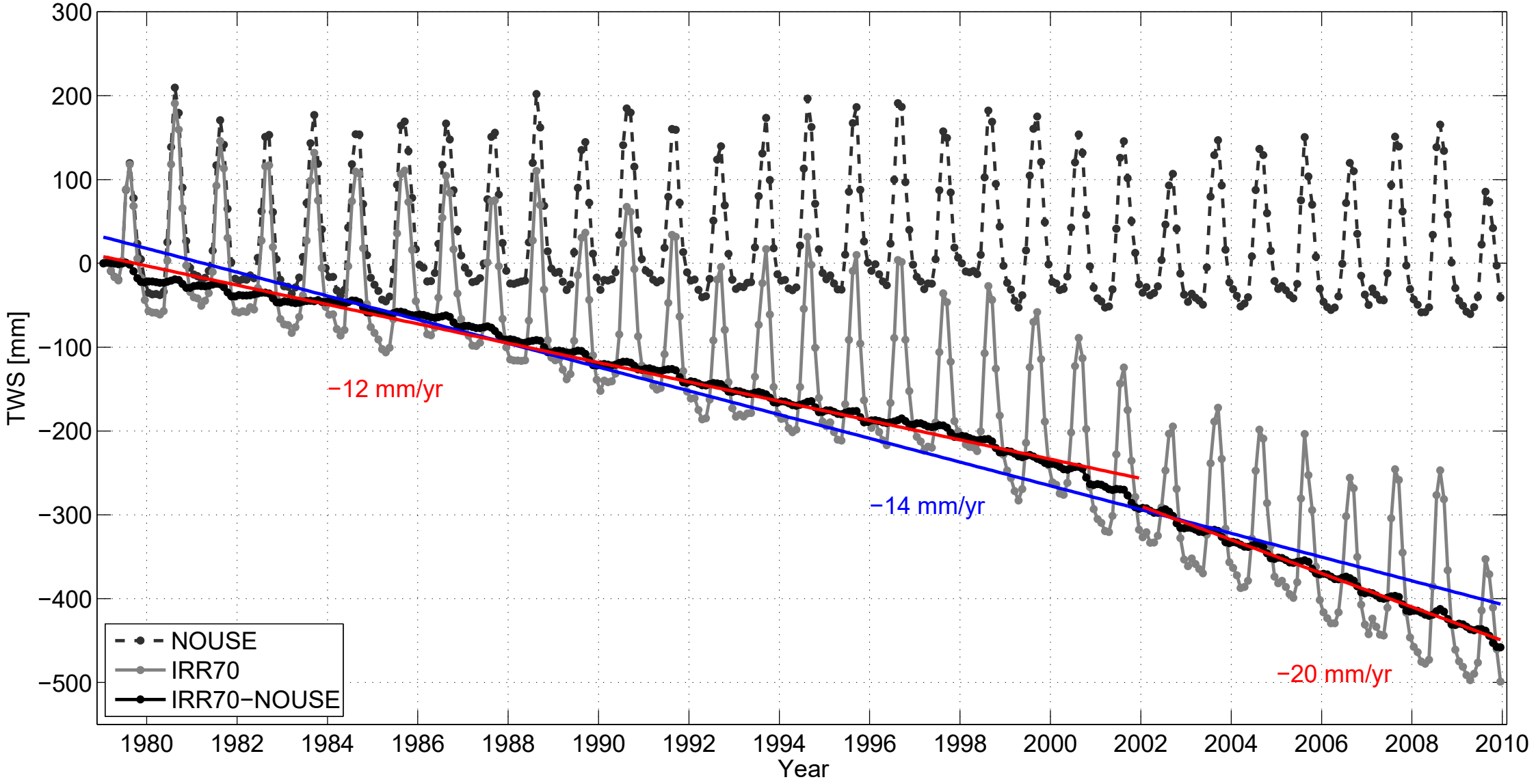
300
200
100
0
−100
−200
−300
−400
−500
TWS [mm]
1980
1982
1984
1986
1988
1990
1992
1994
1996
1998
2000
2002
2004
2006
2008
2010
Year
−12 mm/yr
−14 mm/yr
−20 mm/yr
NOUSE
IRR70
IRR70−NOUSE

Supporting Information for

Exploring the influence of precipitation extremes and human water use on total water storage (TWS) changes in the Ganges-Brahmaputra-Meghna River Basin

Khandu[1,2], E. Forootan[1,3], M. Schumacher[3], J.L. Awange[1,2,4], H. Müller Schmied[5,6]

[1]*Western Australian Centre for Geodesy and the Institute for Geoscience Research, Curtin University, Western Australia, Australia*
[2]*Department of Cartographic Engineering, Universidade Federal de Pernambuco, Recife, Pernambuco, Brazil*
[3]*Institute of Geodesy and Geoinformation, University of Bonn, Bonn, Germany*
[4]*Karlsruhe Institute of Technology, Karlsruhe, Germany*
[5]*Institute of Physical Geography, Goethe-University Frankfurt, Frankfurt, Germany*
[6]*Biodiversity and Climate Research Centre (BiK-F) & Senckenberg Research Institute and Natural History Museum, Frankfurt, Germany*

1. Outline

In this supporting material, various soil moisture products are compared in terms of their seasonal and interannual variability covering the period 1980 to 2014.The soil moisture products and their descriptions are provided in Table S1. It should be mentioned here that soil moistures differ strongly among the various products as these products use different land surface/hydrological models to calculate soil moisture contents over varying soil depths and with varying number of soil layers. We have also included WGHM soil moisture from IRR_70S (variant).

Table S1: Summary of the soil moisture products used in the study.

Products	Spatial resolution	No. of layers	Total depth (m)	References
CPC (reanalysis)	0.50°×0.50°	1	1.60	*van den Dool et al.* (2003)
MERRA (reanalysis)	0.50°×0.67°	1	~1.00	*Rienecker et al.* (2011)
ERA-Interim (reanalysis)	0.79°×0.79°	4	2.55	*Dee et al.* (2011)
Noah (GLDAS)	0.25°×0.25°	4	2.00	*Chen et al.* (1996); *Rodell et al.* (2004)
Mosaic (GLDAS)	0.25°×0.25°	3	3.50	*Koster and Suarez* (1996); *Rodell et al.* (2004)
VIC (GLDAS)	0.25°×0.25°	3	2.00	*Liang et al.* (1994); *Rodell et al.* (2004)
WGHM	0.50°×0.50°	1	land cover dependent, mostly 1 m here.	*Alcamo et al.* (2003); *Döll et al.* (2003); *Müller Schmied et al.* (2014)

2. Results of soil moisture comparison

Soil moisture data sets vary considerably between the different products. The annual range is largest (smallest) in CPC, Noah, and Mosaic (ERA-Interim) (Figure S1). However, soil moisture data sets from three GLDAS land surface models are found to contain spurious jumps between 1995 and 1997 (Figure S3). Soil moisture variability from WGHM appears to be substantially lower than those shown by the others products due to its relatively low available soil water capacity (around 100 mm in the study regions). Since soil moisture of WGHM can range only between wilting point and field capacity (Müller Schmied et al., 2014), it tends to limit the overall seasonal and interannual variation (see, Figures S2 and S4).

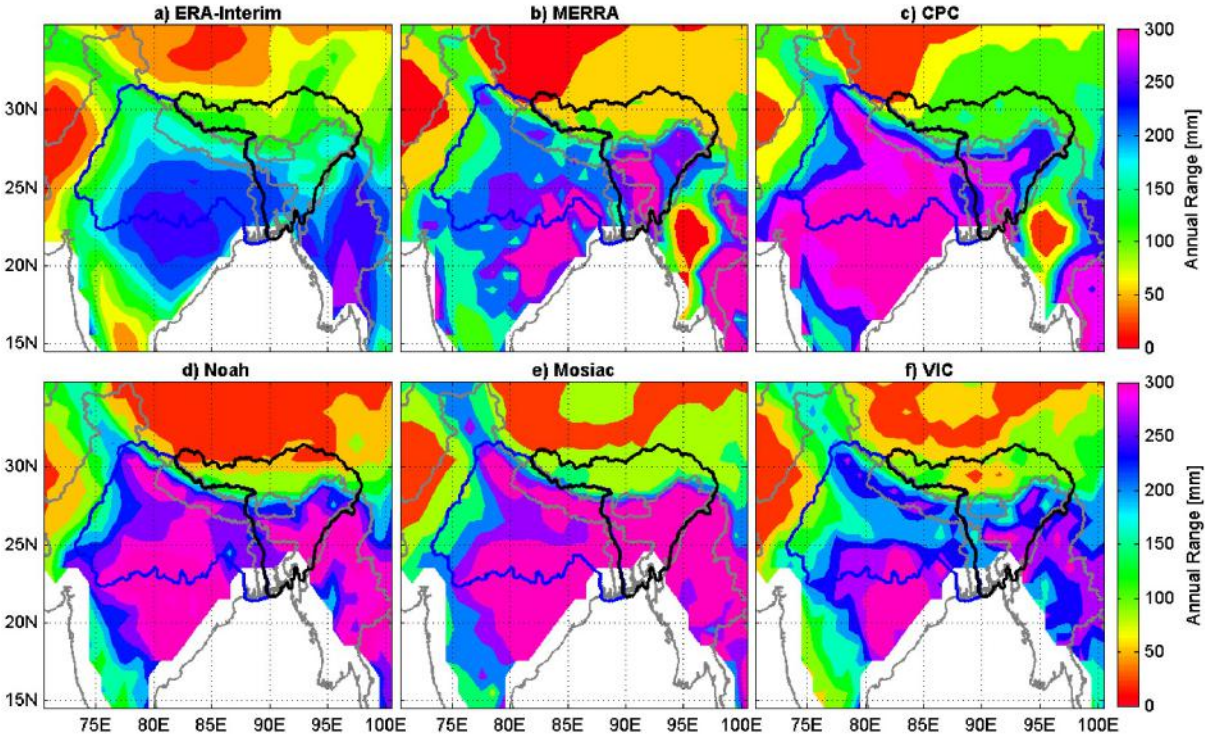

Figure S1: Mean annual range of soil moisture contents (mm) for (a) ERA-Interim, (b) MERRA, (c) CPC, (d) Noah, (e) Mosaic, and (d) VIC covering the period 1980-2014. The annual range is defined as the difference between maximum and minimum soil moisture for every year. CPC, Noah, and Mosaic indicate the highest annual range, while ERA-Interim shows the lowest annual range showing the largest magnitude of about 240 mm in the southern Ganges River Basin.

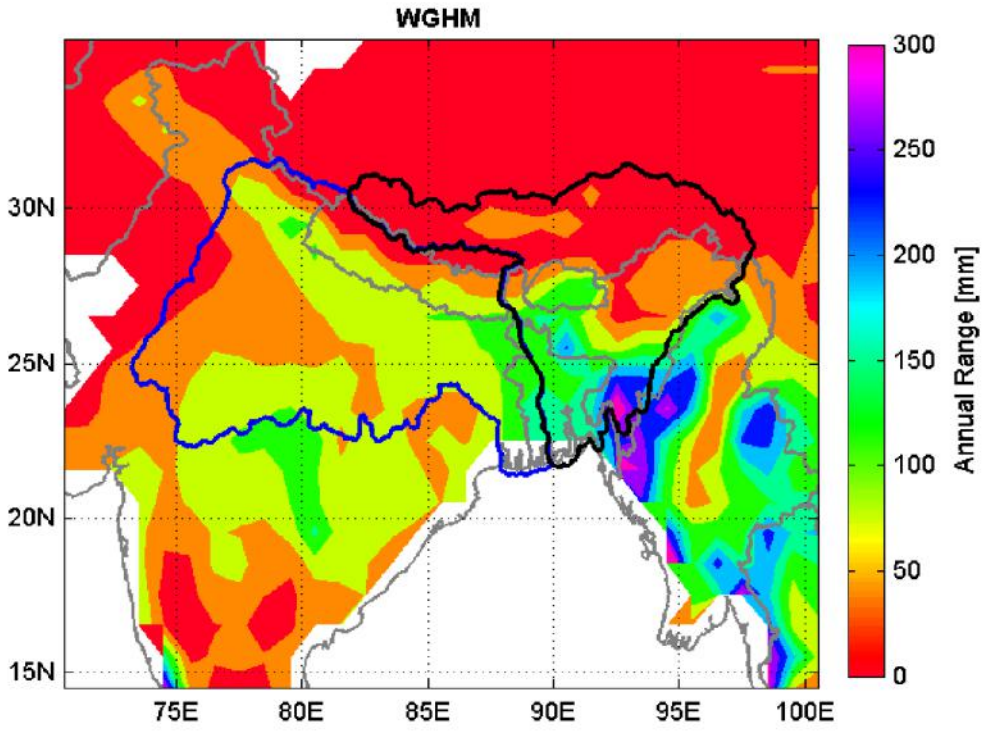

Figure S2: Mean annual range of soil moisture contents (mm) of WGHM covering the period 1980-2009. The results are based on the model variant "IRR_70S". The annual range is significantly lower than those shown in Figure 1 but the spatial patterns are comparable to the other models of Figure S1 in the GBM River Basin.

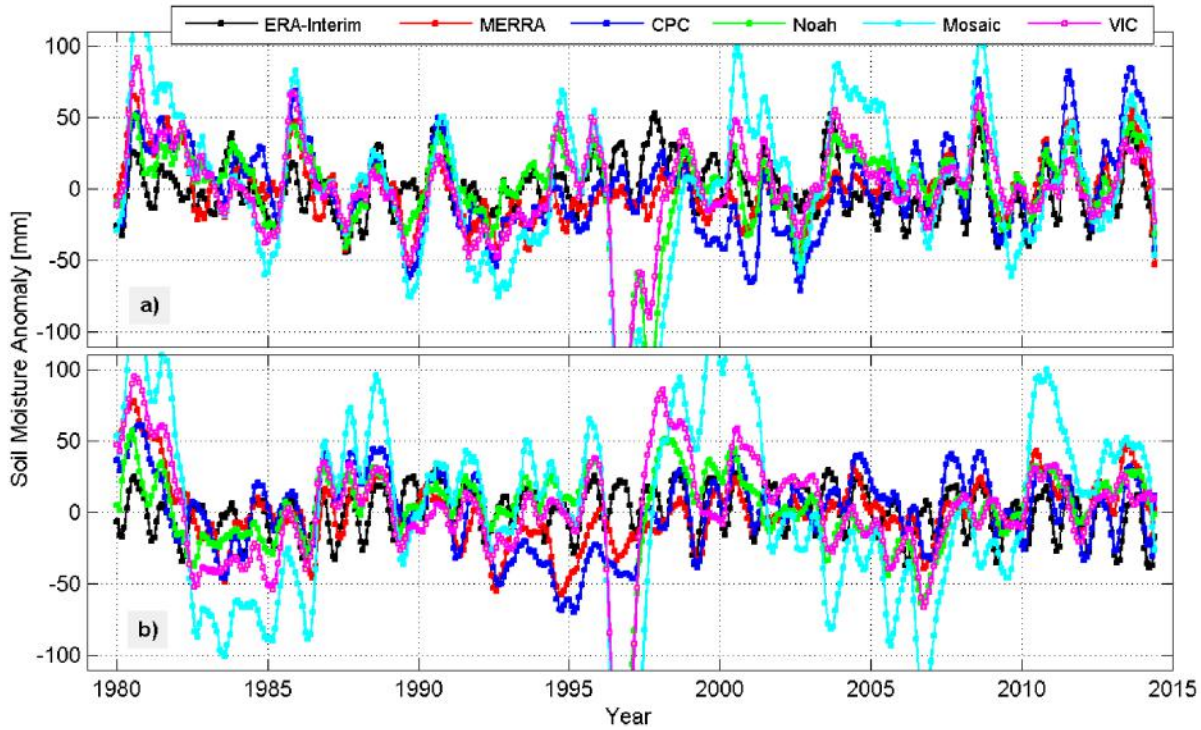

Figure S3: Basin–averaged interannual variation of soil moisture contents from various products in the two river basins: (a) Ganges, and (b) Brahmaputra–Meghna. The anomalies are computed from soil moisture outputs from three reanalyses and three GLDAS land surface models (see Table S1) over the period 1980 to 2014.

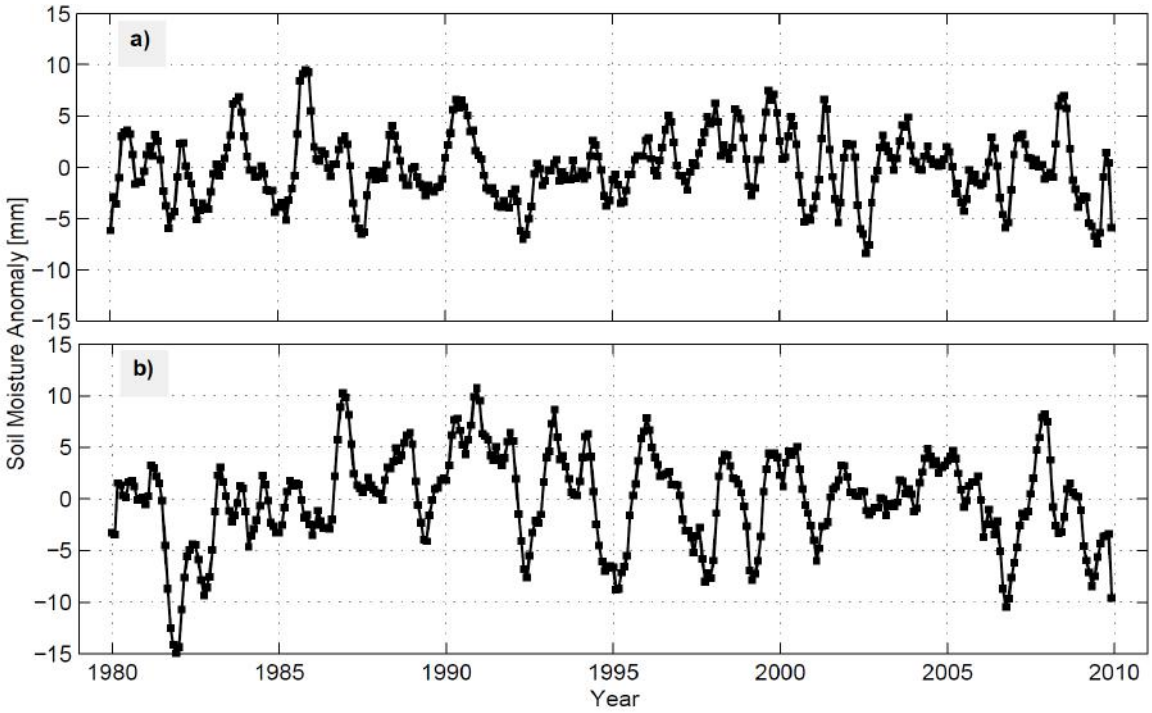

Figure S4: Basin–averaged interannual variation of WGHM soil moisture contents in the two river basins: (a) Ganges, and (b) Brahmaputra–Meghna. The anomalies are computed over the period 1980 to 2009. Consistent with Figure S2, its interannual amplitudes are also significantly lower than those shown in Figure S3**.**

3. References

Alcamo, J., P. Döll, T. Henrichs, F. Kaspar, B. Lehner, T. Rösch, and S. Siebert (2003), Development and testing of the WaterGAP 2 global model of water use and availability, *Hydrol. Sci. J.*, 48(3), 317–337, doi:10.1623/hysj.48.3.317.45290.

Chen, F., K. Mitchell, J. Schaake, Y. Xue, H.-L. Pan, V. Koren, Q. Y. Duan, M. Ek, and A. Betts (1996), Modeling of land surface evaporation by four schemes and comparison with FIFE observations, *J. Geophys. Res.*, 101, 72517268, doi:10.1029/95JD02165.

Dee, D. P., S. M. Uppala, A. J. Simmons, P. Berrisford, P. Poli, S. Kobayashi, U. Andrae, M. A. Balmaseda, , G. Balsamo, P. Bauer, P. Bechtold, A. C. M. Beljaars, L. van de Berg, J. Bidlot, N. Bormann, C. Delsol, R. Dragani, M. Fuentes, A. J. Geer, L. Haimbergere, S. B. Healy, H. Hersbach, E. V. Holm, L. Isaksen, P. Kållberg, M. Köhler, M. Matricardi, A. P. McNally, B. M. Monge-Sanz, J.-J. Morcrette, B.-K. Park, C. Peubey, P. de Rosnay, C. Tavolato, J.-N. Thépaut, and F. Vitarta (2011), The ERA-Interim reanalysis: Configuration and performance of the data assimilation system, *Q. J. R. Meteorolog. Soc.*, 137, 553–597, doi:10.1002/qj.828.

Döll, P., F. Kaspar, and B. Lehner (2003), A global hydrological model for deriving water availability indicators: model tuning and validation, *J. Hydrol.*, 207, 105–134, doi:10.1016/S0022-1694(02)00283-4.

Koster, R. D., and M. J. Suarez (1996), Energy and water balance calculations in the Mosaic LSM, Tech. Rep. Vol. 9, NASA technical memorandum 104606. Technical report series on global modeling and data assimilation.

Liang, X., D. P. Lettenmaier, E. F. Wood, and S. J. Burges (1994), A simple hydrologically based model of land surface water and energy fluxes for general circulation models, *J. Geophys. Res.*, 99, 14,41514,428, doi:10.1029/94JD00483.

Müller Schmied, H., S. Eisner, D. Franz, M. Wattenbach, F. Portmann, M. Flörke, and P. Döll (2014), Sensitivity of simulated global-scale freshwater fluxes and storages to input data, hydrological model structure, human water use and calibration, *Hydrol. Earth. Syst. Sci.*, 18, 3511–3538, doi:10.5194/hess-18-3511-2014.

Rienecker, M. M., M. J. Suarez, R. Gelaro, R. Todling, J. Bacmeister, E. Liu, M. G. Bosilovich, S. D. Schubert, L. Takacs, G. K. Kim, S. Bloom, J. Chen, D. Collins, A. Conaty, A. da Silva, W. Gu, J. Joiner, R. D. Koster, R. Lucchesi, A. Molod, T. Owens, S. Pawson, P. Pegion, C. R. Redder, R. Reichle, F. R. Robertson, A. G. Ruddick, M. Sienkiewicz, and J. Woollen (2011), MERRA: NASA's Modern-Era Retrospective Analysis for Research and Applications, *J. Clim.*, 24(14), 3624–3648, doi:10.1175/JCLI-D-11-00015.1.

Rodell, M., P. R. H. U. Jambor, J. Gottschalck, K. Mitchell, C.-J. Meng, K. Arsenault, B. Cosgrove, J. Radakovich, M. Bosilovich, J. K. Entin, J. P. Walker, D. Lohmann, and D. Toll (2004), The Global Land Data Assimilation System, *Bull. Am. Meteorol. Soc.*, 85, 381–394, doi:10.1175/BAMS-85-3-381.

van den Dool, H., J. Huang, and Y. Fan (2003), Performance and analysis of the constructed analogue method applied to US soil moisture applied over 1981-2001, *Geophys. Res. Lett.*, 108(8617), doi:10.1029/2002JD003114.